DESIGN AND ANALYSIS OF PLANAR MONOPOLE ANTENNAS FOR ULTRA WIDE BAND APPLICATIONS

A Thesis submitted in partial fulfillment of the Requirements for the degree of

Master of Technology
In
Electronics and communication Engineering
Specialization: Communication and Networks

By
Durgasi Sudarshan
Roll No: 212EC5166

Department of Electronics and Communication Engineering
National Institute of Technology Rourkela
Rourkela, Odisha, 769008
May 2014

DESIGN AND ANALYSIS OF PLANAR MONOPOLE ANTENNAS FOR ULTRA-WIDE BAND APPLICATIONS

A Thesis submitted in partial fulfillment of the Requirements for the degree of

Master of Technology
In
Electronics and communication Engineering
Specialization: Communication and Networks

By
Durgasi Sudarshan
Roll No: 212EC5166

Under the Guidance of
Prof. Santanu Kumar Behera

Department of Electronics and Communication Engineering
National Institute of Technology Rourkela
Rourkela, Odisha, 769008
May 2014

DEDICATED TO

My parents and beloved sisters

DEPARTMENT OF ELECTRONICS AND COMMUNICATION ENGINEERING

NATIONAL INSTITUTE OF TECHNOLOGY, ROURKELA

ROURKELA- 769008, ODISHA, INDIA

CERTIFICATE

This is to certify that the work in this thesis entitled **DESIGN AND ANALYSIS OF PLANAR MONOPOLE ANTENNAS FOR ULTRA-WIDE BAND APPLICATIONS** by **Durgasi Sudarshan** is a record of an original research work carried out by his during 2013-2014 under my supervision and guidance in partial fulfilment of the requirement for the award of the degree of Master of Technology in Electronics and Communication Engineering (Communication and Networks), National Institute of Technology, Rourkela. Neither this thesis nor any part of it, to the best of my knowledge, has been submitted for any degree or diploma elsewhere.

Place: NIT Rourkela **Dr. Santanu Kumar Behera**

Date: 27th May 2014 **Associate Professor**

DEPARTMENT OF ELECTRONICS AND COMMUNICATION ENGINEERING

NATIONAL INSTITUTE OF TECHNOLOGY, ROURKELA

ROURKELA- 769008, ODISHA, INDIA

DECLARATION

I certify that

a) Under the supervision of my supervisor the work is done and work in this thesis is original and is done by myself.
b) The work has not been submitted to any other institute for any degree or diploma.
c) For writing the thesis I followed the institute
d) I have given credit to materials when i used them in the thesis and their details are given in the references.

Durgasi Sudarshan
27th May 2014

ACKNOWLEDGEMENTS

The work posed in this thesis is by far the most substantial attainment in my life and it would be unimaginable without people who affirmed me and believed in me. First and foremost I evince my profound reverence and deep regards to my guide **Prof. S. K. Behera** for exemplary guidance, supervising and constant encouragement throughout the course of this thesis. A gentleman embodied, in true form and spirit, I consider it to my good fortune to have consociated with him.

I would like to evince a deep sense of gratitude to estimable **Prof. S. Meher,** Head of the Department of Electronics and Communication Engineering for providing us with best facilities and his timely suggestions.

My special thanks to **Prof. S K. Patra, Prof. K. K. Mahapatra** of Department of Electronics and Communication Engineering for their constant inspiration and encouragement during my research. I want to thank all other faculty members of Department of Electronics and Communication Engineering for their constant support and encouragement during my research. My special thanks to Ph.D scholars Yogesh Kumar Choukiker, Natarajamani S for their help, cooperation and encouragement. I would like to thank all my friends especially Ragasudha Narapaneni who made my journey at NIT Rourkela an indelible and gratifying experience.

My special thanks to Prof. K. J. Vinoy of Department of Electrical Communication Engineering at IISC Bangalore for allowing me to do experimental work in IISC Bangalore.

Finally, my heartfelt gratitude towards my family for their tireless support and love throughout my life. They taught me the value of hard work by their own life example. They gave me tremendous support during my stay in NIT Rourkela.

Durgasi Sudarshan

sudarshan.durgasi@gmail.com

ABSTRACT

In this thesis different antenna designs are proposed for Ultra wideband applications. UWB is a short distance radio communication technology that can perform high speed communications with speeds of more than 100Mbps modern communication system requires a single antenna to cover several wireless bands. The UWB systems have received greater attention in indoor and handheld wireless communication after the allocation of 3.1- 10.6 GHz by the Federal Communications Commission (FCC) for UWB applications. By deploying multiple antennas for transmission an array gain and diversity gain can be accomplished, therefore, the spectral efficiency and reliability is increased significantly and an increase in channel capacity without costing the additional bandwidth or transmit power. MIMO antenna systems require high isolation of less than -16 dB between antenna ports and a compact size for applications in portable devices. This thesis concentrates on the analysis and design of single patch and MIMO antennas with a compact planar profile that have an operating range in the entire UWB (3.1- 10.6 GHz) by having two notch bands for narrow band applications. Some narrow band applications like WiMAX, WLAN etc. can cause interference to the UWB antenna system. The desired antenna performance characteristics are also analyzed.

This thesis presents the work on the design of single element and two element (MIMO) antennas. The proposed designs are analyzed for different performance parameters separately. First, a compact lotus shaped planar monopole antenna is proposed and extended by creating two slots for dual notch performance for narrow band applications. The presented antenna fabricated on a $44\times38\times1.58mm^3$ on thick FR4 substrate and covers the frequency range from 2.86 to 14.0 GHz and is fed by 50 Ω Microstrip line. The extended work of proposed antenna covers the wide range 2.8 to 11 GHz with notch frequencies at 3.458 and 5.51GHz ranging from 3.35GHZ-3.566GHz and 5.285GHz-5.771GHz frequencies.

Second, a two element compact UWB MIMO Antenna systems are designed on an FR4 substrate of dimensions $44\times88mm^2$ of a thickness 1.6mm with lotus shaped elements and antennas are placed in three different angular positions on the substrate. A fork-shaped structure is introduced in the ground plane to increase the isolation between the antennas. Simulated results of S-parameters of the proposed antenna system are obtained and a high isolation of less than -15 dB is achieved throughout the band and it is quite suitable for MIMO applications. The

extended work carried out on creating a dual notch for the different designs placed in three different positions for narrowband applications. The high isolation of less than -15 dB is achieved throughout the band and notch frequencies are situated at 3.44GHz and 5.375GHz by covering WiMAX and WLAN narrow band applications. Among three the antenna placed parallel on a substrate is fabricated and measured. The measured results are well matched to the simulated results.

CONTENTS

NOMENCLATURE

S/N	Signal to Noise ratio
C	Capacity
B	Bandwidth
ε	Dielectric Constant
ε_r	Relative Dielectric Constant
ε_{reff}	Effective Dielectric Constant
L/h	Length to height ratio of Microstrip antenna
W/h	Length to height ratio of Microstrip antenna
Z_0	Characteristic Impedance of a Transmission line
Ω	Ohm
G	Conductance
dBi	Decibel with respect to isotropic antenna
tanδ	Loss tangent
ω	Angular frequency
λ	Wavelength
μ	Permeability
σ	Conductivity
θ	Angle
ρ	Resistivity
η	Efficiency
E	Electric Field intensity Vector
H	Magnetic Field intensity Vector
D	Electric Flux density Vector
B	Magnetic Flux Density Vector
J_C	Conduction Current Density Vector

ABBREVIATIONS

UWB	Ultra Wide Band
FCC	Federal Communications Commission
WiMAX	Worldwide Interoperability for Microwave Access
WLAN	Wireless Local Area Network
CDMA	Code Division Multiple Access
GSM	Global System for Mobile communications
DCS	Personal Digital Cellular
PDC	Personal Digital Cellular system
IS	Interim Standard
Wi-Fi	Wireless Fidelity
IC	Integrated Circuits
NLOS	Non-Line of Sight
LNA	Low Noise Amplifier
MIMO	Multiple-Input Multiple-Output
PIFA	Planar Inverted- F Antenna
PICA	Planar Inverted Cone Antenna
EBG	Electronic Band Gap
USB	Universal Serial Bus
FDTD	Finite Difference Time Domain
CST	Computer Simulation Technology
VSWR	Voltage Standing Wave Ratio
RFID	Radio-frequency identification
CPW	Coplanar Waveguide
SIMO	Serial Input Multiple Output
MISO	Multiple Input Serial Output
SISO	Serial Input Serial Output
SM	Spatial Multiplexing
ITU	International Telecommunication Union
WCDMA	Wideband Code Division Multiple Access

TARC	Total Active Reflection Coefficient
AUI	Antenna Under Test
IF	Intermediate Frequency
LO	Local Oscillator

LIST OF FIGURES

CHAPTER 1

INTRODUCTION

Antenna "The eyes and ears in space" is experiencing a various changes from earlier long wire type for radio broadcast, communication links to the military applications, aircraft, radars, missiles, space applications in the second half of last century. This scenario is fast changing with the evolution of Cellular mobile personal communication in the form of Global System for Mobile communications (GSM), Code Division Multiple Access (CDMA), Digital Communication System (DCS) 1800 systems, North American dual-mode cellular system Interim Standard (lS)-54, North American IS-95 system, and Japanese Personal Digital Cellular (PDC) system etc. The broadband mobile personal communication with high quality mobile video is the bombilate word today. 3rd Generation GSM (3G), Wideband-CDMA, Wireless Fidelity (Wi-Fi), 4th Generation WiMAX, WI Bro, Wire1ess-LAN are all towards this direction.

The antenna does not become obsolete since they are based on constant physical principles. Only technology changes merely like transition from tubes to transistor and then to ICs. Microstrip revolution encountered in antenna technology in 1970s. Antenna the vital part of wireless gadgets have persisted refurbishment from a simple metal rod to ceramic chip, reconfigurable, active and complicated Smart Antenna. The day is not far when this is likely to reduce to physically sub miniature wavelength antennas with the advent of Metamaterials and Nano Technology. In this scenario development of extremely compact antenna are highly relevant Different types of compact antennas like Microstrip, Planar Inverted- F Antenna (PIFA), Planar Inverted Cone Antenna (PICA), Dielectric Resonator Antenna (DRA) and Printed Monopole Antenna.

Ultra-wideband (UWB) technology

Ultra-wideband (UWB) technology for communications and radar has been a topic of research since the early 1960s. However, research and development in this area gained momentum only in recent years for several reasons. The principal reason is the handiness of high-speed semiconductor switching device technology. Another reason is that these systems were ratified for the first time only in 2002 for unlicensed use under the Federal

Communications Commission Part 15 (Title 47 of the Code of Federal Regulations) [FCC. 2002]. The use of UWB in the range of 3.1 to 10.6 GHz was unlicensed by FCC [1]. This permitted the unlicensed use of deliberate UWB wireless emissions within restricted frequency bands at very low power spectral density and is history from the viewpoint of frequency overlay. Finally, as the wireless spectral bands are getting herded with the development of wireless devices, the need for high-bandwidth wireless communications is also forcing the development of UWB communication systems.

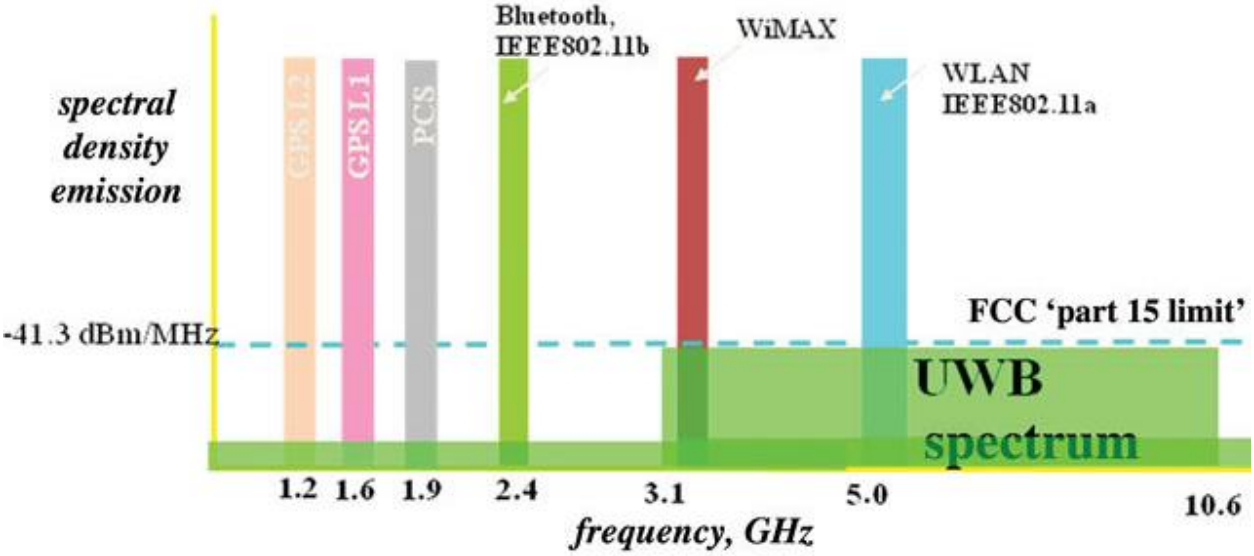

Figure 1. 1 UWB Spectrum

UWB is any radio transmitter with a spectrum that engages more than 20% of the centre frequency or a minimum of 500 MHz and that meets the power limits allotted by the regulatory bodies to minimize the menace to legacy systems. UWB draws gains of broad spectrum in terms of the bit rates it can handle. By Shannon's theorem, the channel capacity C is given by,

$$C = B.\log_2(1 + \frac{S}{N}) \qquad (1)$$

where B is the bandwidth and $\frac{S}{N}$ is the signal-to-noise ratio. Range of operation of such systems is ascertained by the Friis formula.

$$d \propto \sqrt{\frac{P_t}{P_r}} \qquad (2)$$

d being the distance, P_t the transmitted power and P_r the received power, the above equations suggests that channel capacity can be increased by increasing bandwidth instead of power.

Thus, UWB has primarily been a high bit, short range system. The advantages, disadvantages and applications of UWB are listed in Table. 1

Table 1. UWB advantages, disadvantages and applications

UWB Property	Advantages	Disadvantages	Applications
Very wide fractional and absolute bandwidth Very short pulses Persistence of multipath reflections Carrier-less transmission	High rate communications Potential for processing gain Low frequencies penetrate walls, ground Direct resolvability of discrete multipath components Diversity gain Low fade margins Low power Hardware simplicity Small hardware	Potential interference to/from existing systems Large number of multi-paths Long synchronization times Scatter in angle of arrival Inapplicability of super-resolution beam forming	High-rate Wireless Personal Area Network Low-power, communications, indoor localization Multiple access Low power combined communications and localization NLOS (non-line of sight) communications, indoor and on ships Smart sensor networks

Thesis Motivation

The prospective of UWB technology is tremendous on account of its various advantages such as the capability of providing high speed data rates at short distance transmission with low power dissolution. The rapid growth in wireless communication systems has made UWB is an outstanding technology because of accelerated advances in wireless communication systems to replace the conventional wireless technologies at present like Bluetooth and wireless LANs, etc. To develop UWB LNAs, mixers and entire front-ends a lot of research has been done but not that much appreciable to develop UWB antennas. Recently, the tradeoffs between antenna design and transceiver complexity have been realized academic and industrial communities. In general, the transceiver complexity is increased, with the intromission of advanced wireless transmission techniques. In order to increase the performance of the transceiver without compromising on its architecture cost, the antenna design should be made in such a way that the antenna is an inherent part of the transceiver. Also, the ramification of the overall transceiver is reduced [2].

To implement UWB technology, there is a need to overcome many challenges. It has a surge of concern in antenna design by allowing new challenges and chances for antenna designers as UWB systems require an antenna with an operating bandwidth covering the entire UWB (3.1-10.6 GHz) and capable of receiving on colligated frequencies at the same time [3]. Moreover, UWB is a technology that modulates nano pulses based waveforms rather than continuous carrier waves. Hence, the design of UWB antennas requires different considerations from those used in designing narrow band antennas. To accomplish a wide impedance bandwidth with high radiation efficiency is the biggest challenge in designing a UWB antenna. UWB antennas attain, greater than 100% of the center frequency bandwidth, to ensure sufficient impedance so that only less than 10 % of incident signal is lost because of reflections caused at the antenna input terminal [3]. In order to incur high radiation efficiency, greater than 10 dB return loss is essential. It is expected as UWB transmission is of very low power (below the noise floor level) and with high sensitivity [2].

There is increase in demand for small and low cost UWB antennas that are capable of providing acceptable performance in both time and frequency domains. The UWB based systems, are to build small, low-profile integrated circuits so as to be suitable to portable wireless devices. The size affects the gain and bandwidth. So, the size of the antenna is conceived as one

of the vital parameter in the design of UWB system. The volume of the UWB antennas can be minimized by the use of planar designs i.e. by replacing three-dimensional radiators with their planar versions. The planar antenna can be printed on a PCB and thus incorporated easily into RF circuits [4]. Some narrow band applications like WiMAX, WLAN etc. can cause interference to the UWB antenna system.

Currently, there is a demand in the increase of data rate in subsisting wireless communication systems. By assuming typically two antennas in a mobile terminal the data rate and reliability can be enhanced by employing the diversity techniques without sacrificing additional spectrum or transmitted power in rich scattering environments. Multiple-Input-Multiple-Output (MIMO) technology has drew attention in modern wireless communication systems. In MIMO systems multiple antennas at the transmitter transmits the same power as of multiple receivers receives the power. Therefore, there is an increase in the channel capacity without the demand of additional bandwidth or power. The channel capacity can further increased by the use of MIMO UWB systems. Mutual coupling between the individual antennas should be as low as possible for an effective MIMO antenna system.

Hence, these design challenges and features are motivation to researchers in study and design of MIMO antennas for accomplishing high channel capacity with less ramification for accomplishing high data rate UWB applications.

Literature Review on UWB antennas

The Microstrip antenna invention first brought by Deschamps, Grieg, Engleman and Lewin in 1960s, but rigorous research work came into picture since 1970s. Many authors like David M. Pozar, James Hall and others who contributed a lot in start of investigations on Microstrip patch antennas. The size, weight, cost, performance, ease of fabrication and aerodynamic profile are constraints in high-performance aircraft, space craft, satellite and missile applications, and low profile antenna and robust antenna are required Microstrip antennas is found a good candidate for these requirements [5]. These antennas are low profile, conformable to planar and non-planar surfaces, simple and inexpensive to manufacture using modern printed-circuit technology, when mounted on rigid surfaces these antennas are mechanically robust. These are compatible with MMIC designs. It is very easy to design an antenna with required resonance frequency, polarization, input impedance. Just by placing some active loads between

the radiating patch and ground plane one can easily design an antenna with variable resonant frequency, radiation pattern and antenna polarization. Recently so many designs with reconfigure antenna characteristics are investigated. [6], [7]-[12].

The primary intention of this thesis is to design microstrip patch antennas those can stop the narrow band applications which will cause interference to ultra-wide band range 3.1GHz to 10.6GHz reported by FCC. For this compact lotus shape design with two slots is chosen to accomplish the appreciable behaviour. Using this design a MIMO antenna system is developed by carrying several studies on MIMO antennas. To reduce the mutual coupling several geometries like the mushroom–shaped EBG structures [13]–[14], defected ground plane structures [15]–[16] have been proposed by inhibiting the ground current flowing between the radiating elements. An isolation of -26dB is accomplished by a slot formed between the monopole and the ground plane in [17], where a two – port compact UWB MIMO antenna for USB Dongle applications is proposed. The impedance bandwidth is from 3.1 to 5.15 GHz. An isolation of < -20 dB is achieved in another UWB Diversity antenna [18], by optimizing the shape of the ground plane and through slots in the radiating elements. The frequency range of operation of the proposed antenna is 3.1–5 GHz. But, both of these antennas [17] and [18] cover only the lower UWB band. In [19], a diversity antenna has been designed to cover the entire UWB, in which stubs are inserted to reduce the mutual coupling. In [10], enhanced isolation is obtained but, complexity and size of the overall antenna system is increased. In [24], the diversity antenna system is designed to achieve the reduced mutual coupling and to cover the entire UWB. In this structure the antennas are placed orthogonally so that to achieve the mutual coupling less than -20dB. To combat the multi-path fading problem in wireless communication systems, antenna diversity techniques that receive and transmit data using the multiple antennas are studied recently [20]. Spatial diversity technique is one where the antennas are placed a part so that the fading can be decreased. [21] - [23].

Thesis Organization

The organization of this thesis is as follows.

Chapter 2: This chapter presents the basic theory of Microstrip antennas, including the basic microstrip patch geometries, features, different feeding methods describing their characteristics, the advantages and disadvantages of Microstrip antennas. Different calculations are shown to

calculate the feed line width and other dimensions of Microstrip antennas. This chapter ends with brief description on the fundamental an antennas.

Chapter 3: The introductory part of the numerical method, Finite Difference time domain Method (FDTD), which is helpful to analyze any complex geometry. This chapter ends with description of Yee cell and stability of the algorithm.

Chapter 4: This chapter describes the designs of Ultra wide band antenna using CST Microwave Studio Suite 12. The simulated results are presented in terms of different antenna parameters such as return loss, gain, radiation patterns for two designs i.e. simple UWB antenna and dual notch UWB antenna.

Chapter 5: In this chapter the basic theory regarding MIMO technology. Different UWB MIMO antennas systems are designed by employing without dual notch and with two notches and also described. The simulated results are presented in terms of different antenna parameters such as return loss, gain, radiation patterns for different designs. Performance parameters like envelope correlation coefficient, total active reflection coefficient and capacity loss are discussed and simulated results are presented. Designs are simulated using CST Microwave Studio Suite 12. Measured results are presented for two antenna systems which shows that the measured results are well matched to simulated results.

Chapter 6: This chapter contains conclusion and scope of future work

CHAPTER 2

MICROSTRIP ANTENNA

This chapter deals with the basics of microstrip antennas, the advantages and disadvantages. The basic geometries, feeding techniques, features and applications of planar antennas are exemplified here. The fundamental parameters of the antenna are discussed here.

Introduction to Microstrip patch Antenna

The thought of microstrip antenna was traced in 1953 [25] and a patent in 1955 [26]. But it gained significant attention in the start of 1970s. High performance application where weight, size installation and robustness is the main requirement microstrip antenna is used such as aircraft, space craft, automobile vehicles, and satellite and missile applications. The antennas discussed earlier are 3-dimensional antennas which are bulky and need more space to be deployed. Microstrip antennas are used to meet these requirements [5]. The demand for compact and low-cost antennas has brought the microstrip antenna to the forefront due to gaining demand for personal and hand held mobile communications. Microstrip antennas are also called as patch antennas as radiating patch. One of the major advantages is that we can fabricate the feeding and matching networks with the radiating patch on the dielectric substrate. The ground plane is placed on the back side of the substrate. The top and side views of a rectangular microstrip antenna are shown in Fig. 2.1. The radiating patch may be square, circular, elliptical, circular ring, ring sector shapes etc. shown in Fig. 2.2. Because of ease of fabrication, analysis and attractive radiation properties the rectangle and circular patches are frequently used. They are having low cross-polarization radiation.

The basic properties of microstrip patch antennas have been numerously discussed in literature [27], [28].

The different types of radiators are broadside and end-fire radiator. Broadside radiators have its maximum radiation pattern directed normal to the patch or axis of the antenna element. The end-fire radiators have its maximum radiation pattern directed along the axis of the antenna element. The maximum pattern of the patches is normal to the patch i.e. in general it acts as broadside radiator. By properly choosing the mode i.e. field configuration of the excitation under

the patch, the broadside radiator pattern can be achieved. By judicious mode selection, the End-fire radiation can be achieved. The strip and ground plane are separated

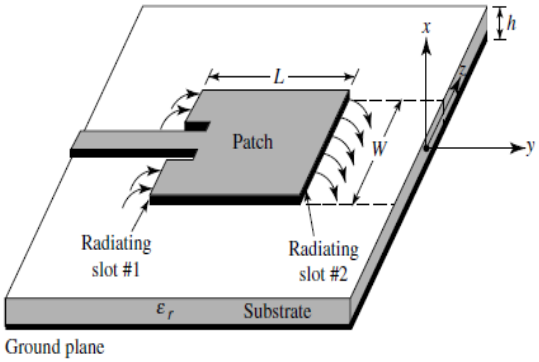

(a) Microstrip antenna

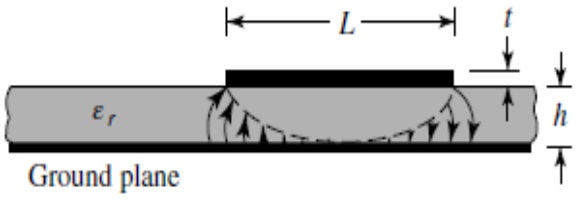

(b) Side view

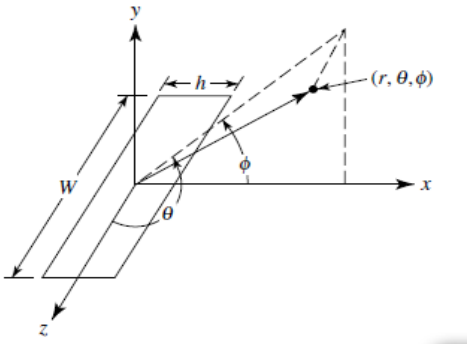

(c) Coordinate system for radiating slot

Figure 2. 1 Microstrip antenna and its side view

by a dielectric sheet as shown in Fig. 2.1.

There are varieties of dielectric material that can be used as substrates in microstrip antenna design with the dielectric constant in the range of $2.2 \leq \varepsilon_r \leq 12$. For designing an antenna with good efficiency, larger bandwidth the substrate height should be more and its dielectric constant should be low, because the low dielectric constant material provides loosely bounded fields which leads to release the of more radiation s into space, but it costs in increase of antenna size. While substrate with higher dielectric constants and lower thickness is used in the applications where tightly bounded fields are required such as waveguides and microwave circuitry. But uses of high dielectric constant material will cost in poor efficiency and smaller bandwidths or greater losses [29]. Various types of shapes that used as a microstrip radiating patch are shown in figure below. Rectangular and circular are the most widely used shapes.

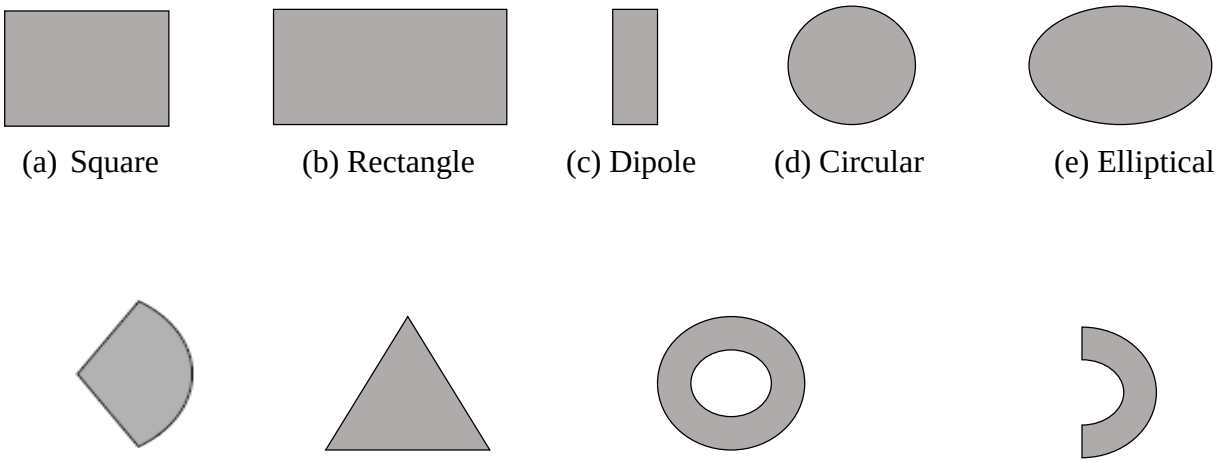

Figure 2. 2 Different shapes of microstrip patch elements.

Feeding Methods

There are different feeding configurations used to feed the microstrip antennas. The four of them which are popularly used [5] are listed below

1. Microstrip or CPW feed line
2. Coaxial probe feed
3. Aperture coupling
4. Proximity or EMC coupling

The microstrip feed line is also a metallic strip has smaller width as compared to that of the patch. The main advantage of using the microstrip line feed is that it is very easy to manufacture one can easily fabricate the fed line with the radiating patch on substrate. It is easy to achieve the impedance matching by feeding at the inset position and also it is very simple to model. However microstrip feed line suffers from surface waves and spurious feed radiation especially when a substrate with high thickness is used, also has the narrow bandwidth (typically 2-5%). A microstrip patch antenna using this feed line is shown in figure with its equivalent circuit in Figs. 2.3 and 2.4, respectively.

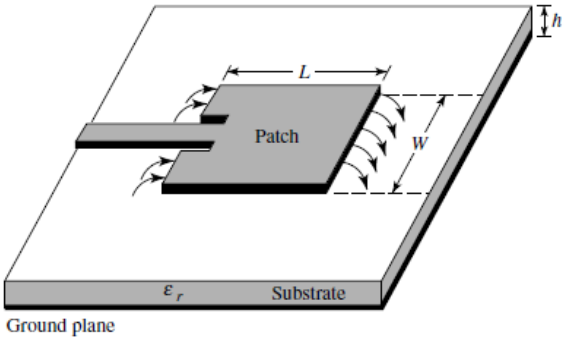

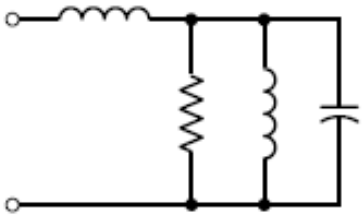

Figure 2. 3 Microstrip line feed **Figure 2. 4** Electrical Equ. Circuit for Microstrip line feed

In the coaxial-line feeding a hole is made in the ground plane and substrate through which the core conductor cable is soldered to the radiating element. While the outer cable of feed line is made connected to the ground plane. The coaxial probe feed can also easy to fabricate but difficulty arises in drilling the core conductor in ground plane and substrate and proper soldering required. Coaxial probe feed has the advantage that a designer can easily get the impedance match by feeding at the driving point (is a point where antenna impedance is equal to characteristic impedance of feeding cable usually 50 ohm). It has low spurious radiation. However, it also has narrow bandwidth and difficult to model. A typical coax feed and its equivalent circuit is also shown in Figs. 2.5 and 2.6 respectively.

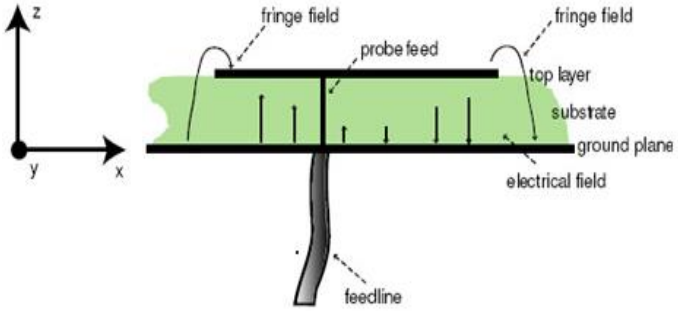

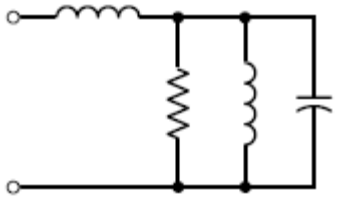

Figure 2. 5 Coaxial line feed **Figure 2. 6** Electrical Equ. Circuit for coaxial line feed

These contacting feeding methods microstrip line and probe feed shows asymmetry which results in generation of the higher order modes. Therefore to avoid this problem, non- contacting feeding are used. The aperture coupled feed is most difficult to fabricate among four feeding techniques. But, it is easy to model and having less unwanted radiation.

Aperture coupling having a ground plane sandwiched between two substrates. The slot is made on ground plane to couple the energy from feed line to patch. Various types of shapes are used in this feed. Rectangular shape is mostly used of them. Lower substrate has high dielectric

material for tightly bounding the fields. The selection of substrate material plays a major role on antenna performance. The Upper substrate is responsible for releasing the electromagnetic waves into space therefore for better radiations low dielectric material is used as upper substrate. While the lower one supports in coupling the energy from feed line to radiating patch, therefore a thin substrate with higher dielectric constant is used in the lower substrate. The amount of energy coupled to radiating patch depends on the slot dimensions and position, they can be optimize in order to get the maximum coupling optimize. This feed also has low spurious feed radiation. An antenna using aperture coupled feed with its electrical equivalent circuit in Figs. 2.7 and 2.8 respectively.

The Proximity coupling has the advantage of large bandwidth, easy to model and has less unwanted radiation. However it is difficult to fabricate because of proper alignment of feed line and radiating patch is required. As in aperture coupled, proximity coupled feed also uses two substrates which are selected in the same manner as in aperture coupled. Feed line is placed between the substrate and the ground plane is kept below the lower substrate. Feed line is extended a more as a stub.

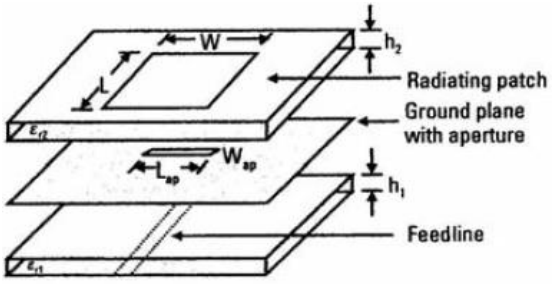

Figure 2. 7 aperture coupled feed

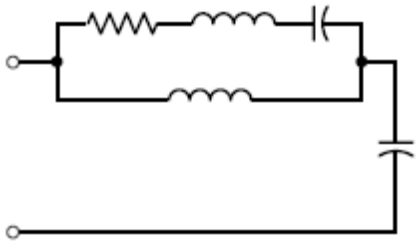

Figure 2. 8 Electrical Equ. Circuit for aperture coupled feed

There are basically two types of bandwidths, impedance bandwidth, defined as the bandwidth over which the antenna remains matched to the feed line to some specified level such as VSWR ≤ 2 and the pattern bandwidth, defined as the bandwidth over which the pattern remains constant. The ideal broadband element will meet both the standards.

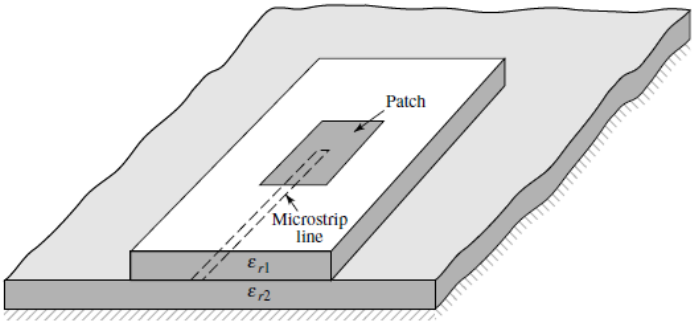

Figure 2. 9 Proximity coupled feed

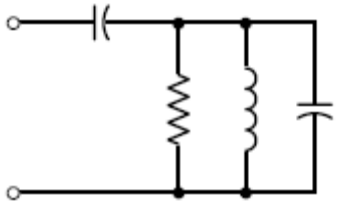

Figure 2. 10 Electrical Equ. Circuit of proximity coupled feed

Analysis of Microstrip antenna

There are different methods to analyze the microstrip antenna. The popular models are transmission line model, cavity model and full wave model. The simplest model of among all is transmission line model. It is easy to analyze using this model and it is more accurate when it employed on thin substrate. The disadvantage of this model is, as it gives less precise results and lacks in versatility. The transmission line model constitutes the microstrip antenna by two slots distinguished by a low-impedance transmission line of length L, width W and height H, as shown in Fig.2.11.

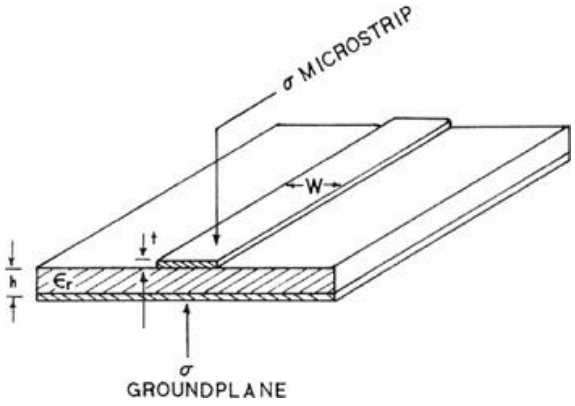

Figure 2. 11 Microstrip line

Fringing Effects

Since the patch dimensions are finite along the length and width, the fields at the patch edges undergo fringing. This is instanced in Fig.2.1 (a, b) for the two radiating slots of the microstrip antenna. The amount of fringing fields coming from the radiating edges mainly depends on the dielectric material used in substrate and the height of substrate. Lower the dielectric constant material results more bowed fringing fields that leads to better radiation. Therefore lower the dielectric material constant better the radiation. For a microstrip line, typical electric field lines are shown in Fig.2.12. It can be observed that the fringing field line are not only travels in substrate but also in the air. Therefore for the more accurate prediction of the performance of antenna the air should also take into consideration. As L/h ratio increases and $\varepsilon_r >> 1$, the fringing field will more concentrate on the substrate. Due to these fringing fields coming out from the edges the operating length becomes more than the physical length. Therefore to consider the fringing effect in patch antenna, an effective dielectric constant (EDC) is calculated [5].

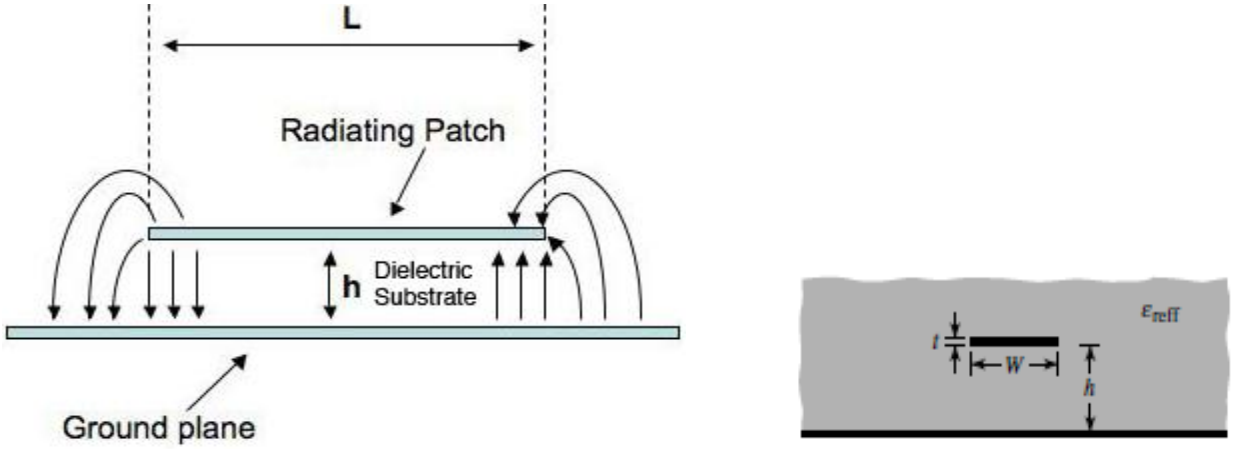

Figure 2. 12 Microstrip Electric field lines and effective dielectric constant

The value of ε_{reff} is nearer to the value of the actual dielectric constant used. The effective dielectric constant is a function of frequency. For the higher frequency the value of effective dielectric constant reaches to the actual value. Effective dielectric constant will be in the range of $1< \varepsilon_{reff} < \varepsilon_r$. As the frequency of operation increases the fringing fields disappears, because the electric field lines will concentrate inside the substrate [5].The graph showing in fig. 2.13 the variation of ε_{reff} value with frequency for three different types of materials.

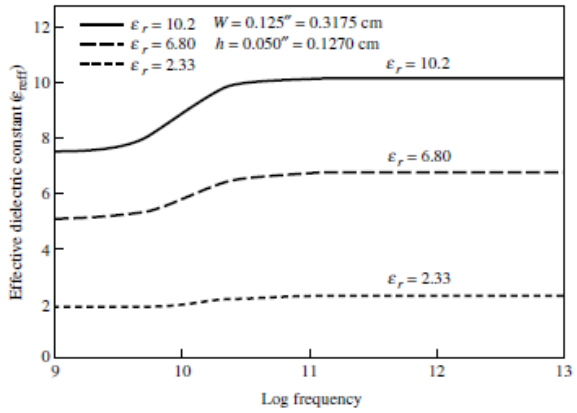

Figure 2. 13 Effective dielectric constant vs. frequency for different substrates

For low frequencies, effective dielectric constant is almost constant. At the intermediate frequencies its values start to gain slowly and finally approach the values of the actual value of dielectric constant. The initial values also referred to as static values (at lower frequencies) of effective dielectric constant is given by Eq. 2.1. This value is sensible for W/h > 1.

$$\varepsilon_{reff} = \frac{\varepsilon_r + 1}{2} + \frac{\varepsilon_r - 1}{2}\left(\frac{1}{\sqrt{1+\frac{12h}{W}}}\right) \qquad (2.1)$$

where W is width of feed line and 'h' is height of the substrate.

The dimensions of the patch along its length have been extended on each end by a distance ΔL as depicted in Fig.2.14. It is function of ε_{reff} and W/h. The practical approximate relation to length for its normalized extension is given in Eqs.2.2 and the effective length of the patch is in 2.3.

$$\frac{\Delta L}{h} = 0.412\frac{\left(\varepsilon_{reff} + 0.3\right)\left(\frac{W}{h} + 0.264\right)}{\left(\varepsilon_{reff} - 0.258\right)\left(\frac{W}{h} + 0.8\right)} \qquad (2.2)$$

$$L_{eff} = L + 2\Delta L \qquad (2.3)$$

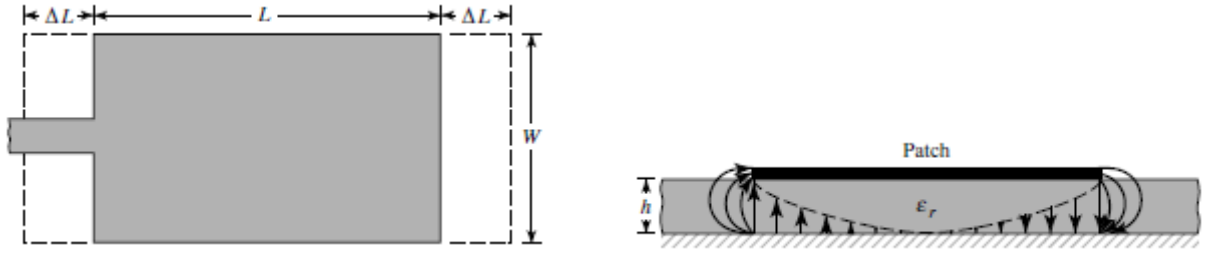

(a) Top view (b) Side view

Figure 2. 14 Physical and effective lengths of rectangular microstrip patch

The characteristics impedance **Z_0** of the microstrip feed line depends on the width **W** of the feed line and height **h** of the substrate and it holds different values for W/h ≤ 1 and W/H ≥ 1 as exemplified in the Eqs.2.4 and 2.5 respectively.

$$Z_0 = \frac{60}{\varepsilon_{reff}} \ln\left[\frac{8h}{W_0} + \frac{W_0}{4h}\right], \qquad \frac{W}{h} \le 1 \qquad (2.4)$$

$$= \frac{120\pi}{\sqrt{\varepsilon_{reff}}\left[\frac{W_0}{h} + 1.393 + 0.667\ln\left(\frac{W}{h} + 1.444\right)\right]}, \qquad \frac{W}{h} \ge 1 \qquad (2.5)$$

The width **W** of the line and height **h** of the substrate is decided by parameters A and B which are functions of the characteristic impedance of the line and dielectric constant of the substrate as shown in Eqs.2.6, 2.7, 2.8 and 2.9.

$$\frac{W}{h} = \frac{8e^A}{e^{2A} - 2}, \qquad \frac{W}{h} < 2 \qquad (2.6)$$

$$\frac{W}{h} = \frac{2}{\pi}\left[B - 1 - \ln(2B-1) + \frac{\varepsilon_r - 1}{2\varepsilon_r}\left\{\ln(B-1) + 0.39 - \frac{0.61}{\varepsilon_r}\right\}\right], \qquad \frac{W}{h} > 2 \qquad (2.7)$$

Where

$$A = \frac{Z_0}{60}\sqrt{\frac{\varepsilon_r + 1}{2}} + \frac{\varepsilon_r - 1}{\varepsilon_r + 1}\left(0.23 + \frac{0.11}{\varepsilon_r}\right), \qquad (2.8)$$

and

$$B = \frac{377\pi}{2Z_0\sqrt{\varepsilon_r}} \qquad (2.9)$$

Generally, the characteristics impedance of the feed line is taken as 50Ω. The reason behind choosing this are described below:

- Practically, all source ports that are available having 50Ω internal impedance. Therefore by Maximum Power Theorem, there is a need to select a feed line of 50Ω characteristic impedance for the microstrip antenna to transfer maximum power from source to load.
- Theoretically, it is determined that 76Ω is required for minimum attenuation in the line and 37Ω is needed for maximum power transfer from the line. Therefor to compromise between these two, we are choosing the average of the above two values i.e. 50Ω as the characteristics impedance for the feed line.

Advantages and Disadvantages of Microstrip antenna

Microstrip patch antenna has various advantages over conventional microwave antenna with one similarity of frequency range from 100 MHz to 100 GHz. There are enormous number of advantages and having few disadvantages also.

Advantages

Light weight, low volume, low profile.

Printed circuits are thin, therefore they require less volume than their waveguide or coaxial similitudes. Printed circuits antennas consist primarily of nonmetallic materials like foam materials as substrates, such antennas have an extremely low weight compared to conventional antennas.

Polarization

Any polarization can be obtained with the versatility of patch geometries. We can realize multi polarization capability in antennas with single or multiple ports.

Dual frequency antennas

We can realize dual-frequency operation in antennas by employing either dual-stacked patches or a loaded diode or a stub on patch.

Excitation technique

Patches allow a various excitation techniques to be employed, compatible with any technology of the active circuitry and beam forming networks.

Suitable for integration with MICs (Microwave Integrated Circuits)

MICs are in good deal to handle and less expensive than the alternative waveguides.

Disadvantages

a) Narrow bandwidth
b) Low efficiency
c) Low Gain
d) Extraneous radiation from feeds and junctions
e) Poor end fire radiator except tapered slot antennas
f) Polarization purity is difficult to achieve
g) Low power handling capacity.
h) Surface wave excitation

Applications

Since the microstrip antenna having advantages like light weight and ease to design and installation, low cost etc. it is having enormous applications. Initially it brings the applications in military and satellite. Recently, they are extended to commercial applications. Some of the applications are listed below:

a) Mobile and satellite applications
b) Global positioning system
c) Radar applications
d) Medical applications
e) Worldwide Interoperability for Microwave Access (WiMAX)
f) Radio Frequency Identification (RFID)

Fundamentals parameters of Antennas

Various parameters are required to describe the performance of an antenna. definitions of some of are listed below:

Gain and directivity

The gain of an antenna is “the ratio of the intensity, in a given direction, to the radiation intensity that would be obtained if the power accepted by the antenna were radiated equally in all directions” [5]. According to IEEE standards the gain does not include losses arising from reflections and polarization mismatches. The concept of an isotropic radiator is essential to

define the gain i.e. it radiates the power to all directions equally. An isotropic antenna is ideal antenna. However, all practical antennas must have some directional characteristics. The gain of the isotropic antenna is unity (g = 1 or G = 0 dB) in all directions. For estimating antenna gain isotropic antenna is fundamental reference and dipole is another reference used commonly. In this case the gain of an half wavelength dipole is employed. Its gain is 1.64 (G = 2.15 dB) comparitive to an isotropic radiator. The gain of an antenna is usually expressed in decibels (dB). The units are evinced as dBi when the gain calculated by taking the isotropic radiator reference, but when the half-wave dipole considered as reference, the units are conveyed as dBd. The relationship between these units is

$$G_{dBd}G_{dBd} = G_{dBi}G_{dBi} - 2.15dBidB \tag{2.10}$$

Directivity is defined as "the ratio of radiation intensity in a given direction to the radiation intensity averaged over all directions". The effects due to power lost in the antenna are not considered in directivity. The gain of the antenna is same as the directivity (in a given direction) if an antenna is 100% efficient.

Antenna Polarization

The polarization term can be defined as that tip of the electric field traces a path. Polarization may be classified as linear, circular, or elliptical. The electric field at a point in space directed along a line, the field is said to be linearly polarized. A time-harmonic wave is circularly polarized at a given point in space if the electric (or magnetic) field vector at that point traces a circle as. Depends on the orientation of the field it can be categorized as left hand circular polarization and right hand circular polarization. A wave is elliptically polarized if the field vector traces an elliptical locus in space. Depends on the orientation of the field it can be categorized as left hand elliptical and right hand elliptical polarization [5].

Input impedance

Input impedance is defined as "the impedance presented by an antenna at its terminals". The input impedance of patch antenna is generally complex as it includes resonant and non-resonant part. Both real and imaginary parts of the impedance vary as a function of frequency. Ideally, at the resonant frequency both the resistance and reactance exhibit as shown in Figure

2.15.The feed reactance is generally very small relative to the resonant resistance for thin substrates [5].

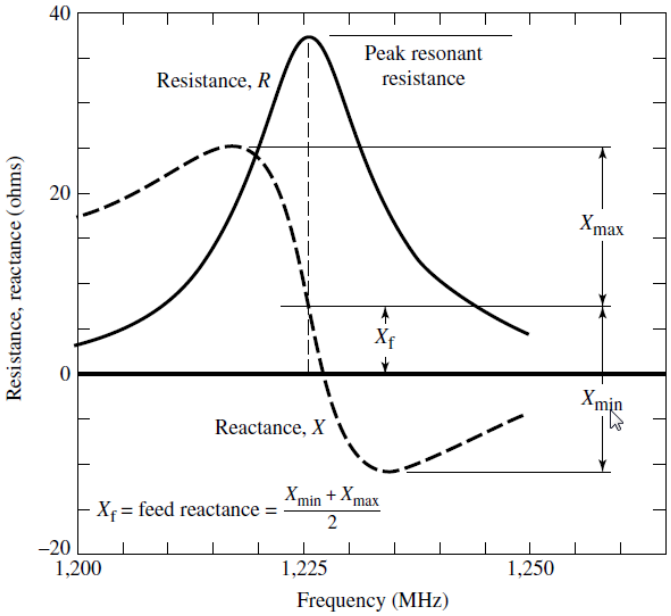

Figure 2. 15 Typical impedance curve of rectangular Microstrip antenna versus frequency

Voltage Standing Wave Ratio

The standing wave ratio (SWR), also known as the voltage standing wave ratio (VSWR), A measure of the mismatch of a line. It can be defined as

$$SWR = \frac{V_{max}}{V_{min}} \tag{2.11}$$

It is a real number ranging from one to infinity. VSWR =1 implies that it's a matched load which is an ideal case. VSWR of 1.5 is considered excellent, while values of 1.5 to 2.0 is considered good and values higher than 2.0 may be unacceptable.

Bandwidth

The bandwidth of an antenna can be defined "as the range of frequency within which the performance of the antenna meets specified standard" which means the characteristics of antenna (gain, radiation pattern and terminal impedance) have satisfactory values within the bandwidth limits.

Bandwidth can be described on the basis of gain, axial ratio bandwidth, and Impedance or VSWR bandwidth. The impedance bandwidth is the range of frequencies in which the input impedance of antenna is perfectly matched to the characteristic impedance of the feeding transmission line. For broadband antennas the ratio of the upper to lower frequencies of acceptable operation is used to express the bandwidth. However, for narrowband antennas, the bandwidth is expressed as a percentage of the bandwidth [5].

Quality factor

The quality factor is useful in determining the VSWR bandwidth of the antenna. Typically there are radiation, conduction, dielectric and surface wave losses.

$$\frac{1}{Q_T} = \frac{1}{Q_r} + \frac{1}{Q_c} + \frac{1}{Q_d} + \frac{1}{Q_{sur}} \tag{2.11}$$

Q_T : Total quality of factor

Q_r : Quality factor due to radiation losses

Q_c: Quality factor due to conduction losses

Q_d: Quality factor due to dielectric losses

Q_{sur}: Quality factor due to surface waves

For very thin substrates $h << \lambda_0$ of arbitrary shapes including rectangular, there approximate formulas to represent the quality factors of the various losses. These can be expressed as

$$Q_c = h\sqrt{\pi f \mu \sigma} \tag{2.12}$$

$$Q_d = \frac{1}{\tan\delta} \tag{2.13}$$

$$Q_r = \frac{2\omega\varepsilon}{h\frac{G_t}{l}} K \tag{2.14}$$

where tan δ is the loss tangent of the substrate material, σ is the conductivity of the conductors associated with the patch and ground plane, G_t/l is the total conductance per unit length of the radiating aperture and k for rectangular microstrip antenna is L/4. For thin substrates, the surface wave losses can be neglected. But need to consider for thick substrates [5].

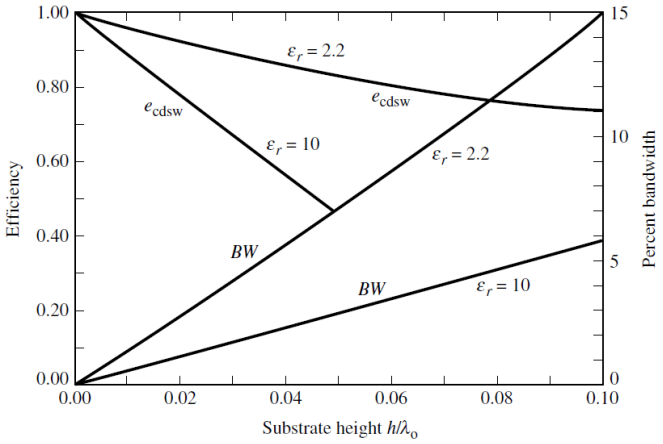

Figure 2. 16 Efficiency and bandwidth versus substrate height at constant resonant frequency for Rectangular Microstrip patch for two different substrates [32].

A typical variation of the bandwidth for a Microstrip antenna as a function of the normalized height of the substrate, for two different substrates, is shown in Figure 2.16. It is apparent that the bandwidth increases as the substrate height increases. However, the radiation efficiency antenna is the ratio of power radiated over the input power and is expressed in Eqn.2.15. Radiation efficiency decreases as normalized height of the substrate increased.

$$\eta = \frac{Q_T}{Q_r} \qquad (2.15)$$

CHAPTER 3

FINITE DIFFERENCE TIME DOMAIN METHOD

Full wave methods

Full wave methods in electromagnetics can be classified in many ways. The main objective is to solve the Maxwell equations with certain boundary and initial conditions. One possible classification uses the form in which Maxwell equations are expressed (Becker et al. 1995). According to this criterion three broad classes can be identified,

- partial differential equations techniques
- variational approaches
- Integral equations techniques.

Another classification takes into account the domain, in which the equations are expressed,

- time or frequency domain
- spatial or spectral (reciprocal space) domain

According to the above schemes, the Method of Moments is an integral equation method and the FEM (Finite Element Method) is a variational approach. Both methods are usually implemented in the frequency domain.

The FDTD method is a full wave time domain differential equation based technique. It is a versatile method that was proposed by Yee (1966) originally for two dimensional problems with metal boundaries. However it did not gain immediate attention for more than a decade mainly due to considerable computer resources requirements and the lack of boundary conditions for open region problems. Initially the FDTD method was applied to scattering problems and subsequently has become best method for solving problems in electromagnetics (Taflove 1995).

The Differential form of Maxwell's equations

The Maxwell equations in charge free regions containing materials without magnetic losses read, where $\vec{E}$, $\vec{H}$ are the electric and magnetic field respectively and$\vec{D}$, $\vec{B}$ are the electric

and magnetic flux density, $\vec{J}_c$ the conduction current. The constitutive relations in a linear isotropic material characterized by a permittivity ε, conductivity σ, permeability μ are;

$$\nabla \times \vec{E} = -\frac{\partial \vec{B}}{\partial t} \quad (3.1)$$

$$\nabla . \vec{D} = 0 \quad (3.2)$$

$$\nabla . \vec{B} = -\frac{\partial \vec{B}}{\partial t} \quad (3.3)$$

$$\nabla \times \vec{H} = \frac{\partial \vec{D}}{\partial t} + \vec{J}_c \quad (3.4)$$

where $\vec{E}$, $\vec{H}$ are the electric and magnetic field respectively and $\vec{D}$, $\vec{B}$are the electric and magnetic flux density, $\vec{J}_c$ the conduction current. The constitutive relations in a linear isotropic material characterized by a permittivity ε, conductivity σ, permeability μ are;

$$\vec{B} = \mu\vec{H} \quad (3.4)$$

$$\vec{J}_c = \sigma\vec{E} \quad (3.5)$$

$$\vec{D} = \epsilon\vec{E} \quad (3.6)$$

Solving for the time derivatives of the Maxwell curl equations

$$\nabla \times \vec{E} = -\mu\frac{\partial \vec{H}}{\partial t} \Leftrightarrow \frac{\partial \vec{H}}{\partial t} = -\frac{1}{\mu}\nabla \times \vec{E} \quad (3.7)$$

$$\nabla \times \vec{H} = \varepsilon\frac{\partial \vec{E}}{\partial t} + \sigma\vec{E} \Leftrightarrow \frac{\partial \vec{E}}{\partial t} = -\frac{1}{\varepsilon}\nabla \times \vec{H} - \frac{\sigma}{\epsilon}\vec{E} \quad (3.8)$$

The above two equations involve vectors. Taking each component a set of six equations is produced

$$\frac{\partial H_x}{\partial t} = -\frac{1}{\mu}\left(\frac{\partial E_z}{\partial y} - \frac{\partial E_y}{\partial z}\right) \quad (3.9a)$$

$$\frac{\partial H_y}{\partial t} = -\frac{1}{\mu}\left(\frac{\partial E_x}{\partial z} - \frac{\partial E_z}{\partial x}\right) \quad (3.9b)$$

$$\frac{\partial H_z}{\partial t} = -\frac{1}{\mu}\left(\frac{\partial E_y}{\partial x} - \frac{\partial E_x}{\partial y}\right) \quad (3.9c)$$

$$\frac{\partial E_x}{\partial t} = \frac{1}{\varepsilon}\left(\frac{\partial H_z}{\partial y} - \frac{\partial H_y}{\partial z}\right) - \frac{\sigma}{\varepsilon}E_x \quad (3.9d)$$

$$\frac{\partial E_y}{\partial t} = \frac{1}{\varepsilon}\left(\frac{\partial H_x}{\partial z} - \frac{\partial H_z}{\partial x}\right) - \frac{\sigma}{\varepsilon}E_y \quad (3.9e)$$

$$\frac{\partial E_Z}{\partial t} = \frac{1}{\varepsilon}\left(\frac{\partial H_y}{\partial x} - \frac{\partial H_x}{\partial y}\right) - \frac{\sigma}{\varepsilon}E_z \quad (3.9f)$$

Yee's Finite Difference Algorithm

The FDTD method is concerned with the numerical solution of expressions derived from above equations [37]. Yee (1966) introduced finite differences for these expressions by dividing the space in Cartesian cells. In three dimensions, the nodes have discrete coordinates (iΔx, jΔy, kΔz) and the time is measured in discrete intervals $t = n \cdot \Delta t$, where i, j, k, n are integers. In this scheme any arbitrary vector function $\overrightarrow{F}$ ($\vec{r}$, t) can be approximated by a discrete valued function $\vec{F}^n$(i, j, k). For each node, there is a corresponding cell where $\vec{H}$ and $\vec{E}$ components reside (Figure 5). Observe that the electric field components are placed in the middle of the edges and the magnetic field components reside in the centres of the faces. It is worth noticing that the spatial offset gives readily a geometric representation of the integral form of Maxwell's equations (Taflove 1995). The computational domain is divided in $N_x \times N_y \times N_z$ cells. Due to the spatial offset, the magnetic field components $H_x(i,j+0.5,N_z+0.5)$, $H_x(i,N_y+0.5,k+0.5)$, $H_y(i+0.5,j,N_z+0.5)$, H_y $(N_x+0.5,j,k+0.5)$, $H_z(N_x+0.5,j+0.5,k)$, $H_z(i+0.5,N_y+0.5,k)$ and the electric field components $E_x(N_x+0.5,j,k)$, $E_y(i,N_y+0.5,k)$, $E_z(i,j,N_z+0.5)$ are not defined. The FDTD equation is shown below for the H_x component. The first equation among six are written using the finite difference operator Δ to express the derivatives:

$$\frac{\Delta H_x}{\Delta t} = \frac{1}{\mu}\left(\frac{\Delta E_y}{\Delta z} - \frac{\Delta E_z}{\Delta y}\right) \qquad (3.10)$$

Yee's Cell

Yee's cell is used for FDTD. The electric and magnetic fields are distributed accordingly.

a) The electric field components are distributed along the edges of the cube.

b) The magnetic field components are distributed along the normal to the face of the cube.

According to Yee's notation, the grid point can be defines in the solution region as

$$(i, j, k) = (i\Delta x, j\Delta y, k\Delta z) \qquad (3.11)$$

and the function as

$$F^n(i, j, k) = F(i\delta, j\delta, k\delta, n\Delta t) \qquad (3.12)$$

where δ is increase in apace and $\delta = \Delta x = \Delta y = \Delta z$, Δt is increment in time and the integers are denoted with i, j, k, n. By applying approximation using central difference for space and time derivatives,

$$\frac{\partial F^n(i,j,k)}{\partial x} = \frac{F^n(i+1/2,j,k) - F^n(i-1/2,j,k)}{\delta} + 0(\delta^2) \tag{3.13}$$

$$\frac{\partial F^n(i,j,k)}{\partial t} = \frac{F^{n+1/2}(i,j,k) - F^{n-1/2}(i,j,k)}{\Delta t} + 0(\Delta t^2) \tag{3.14}$$

Application of Eq. (3.13) to all in Eq. (3.9), the positions E and H components given by Yee about a unit cell of the structure as shown in Fig. 3.1. To comprise Eq. (3.14), the E and H are valuated by using half in time steps [37]. Thus we obtain the approximation in finite difference explicitly for Eq. (3.9) as:

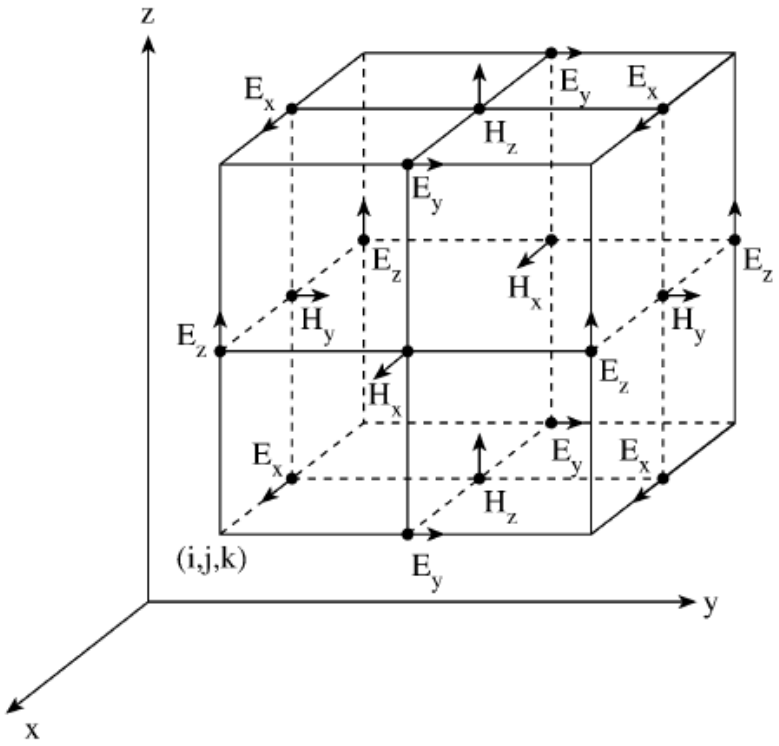

Figure 3. 1 The position of the electric and magnetic field components in an FDTD or Yee cell.

$$H_x^{n+1/2}(i,j+1/2,k+1/2) = H_x^{n-1/2}(i,j+1/2,k+1/2) + \frac{\delta t}{\mu(i,j+1/2,k+1/2)\delta}\begin{bmatrix} E_y^n(i,j+1/2,k+1) - E_y^n(i,j+1/2,k) \\ + E_z^n(i,j,k+1/2) - E_z^n(i,j+1,k+1/2) \end{bmatrix}, \tag{3.15a}$$

$$H_y^{n+1/2}(i+1/2,j,k+1/2) = H_y^{n-1/2}(i+1/2,j,k+1/2) + \frac{\delta t}{\mu(i+1/.2,j,k+1/2)\delta}\begin{bmatrix} E_z^n(i+1,j,k+1/2) - E_z^n(i,j,k+1/2) \\ + E_x^n(i+1/2,j,k) - E_x^n(i+1/2,j,k+1) \end{bmatrix}, \tag{3.15b}$$

$$H_z^{n+1/2}(i+1/2,\, j+1/2,k) = H_z^{n-1/2}(i+1/2,\, j+1/2,k) + \frac{\delta t}{\mu(i+1/2,\, j+1/2,k)\delta}\begin{bmatrix} E_x^n(i+1/2,\, j+1,k) - E_x^n(i+1/2,\, j,k) \\ + E_y^n(i,\, j+1,k) - E_y^n(i+1,\, j+1/2,k) \end{bmatrix}, \tag{3.15c}$$

$$E_x^{n+1}(i+1/2,\, j,k) = \left(1 - \frac{\sigma(i+1/2,\, j,k)\delta t}{\varepsilon(i+1/2,\, j,k)}\right).E_x^n(i+1/2,\, j,k) + \frac{\delta t}{\varepsilon(i+1/2,\, j,k)\delta}\begin{bmatrix} H_z^{n+1/2}(i+1/2,\, j+1/2,k) - H_z^{n+1/2}(i+1/2,\, j-1/2,k) \\ + H_y^{n+1/2}(i+1/2,\, j,k-1/2) - H_y^{n+1/2}(i+1/2,\, j,k+1/2) \end{bmatrix}, \tag{3.15d}$$

$$E_y^{n+1}(i,\, j+1/2,k) = \left(1 - \frac{\sigma(i,\, j+1/2,k)\delta t}{\varepsilon(i,\, j+1/2,k)}\right).E_y^n(i,\, j+1/2,k) + \frac{\delta t}{\varepsilon(i,\, j+1/2,k)\delta}\begin{bmatrix} H_x^{n+1/2}(i,\, j+1/2,k+1/2) - H_x^{n+1/2}(i,\, j+1/2,k-1/2) \\ + H_z^{n+1/2}(i-1/2,\, j+1/2,k) - H_z^{n+1/2}(i+1/2,\, j+1/.2,k) \end{bmatrix}, \tag{3.15e}$$

$$E_z^{n+1}(i,\, j,k+1/2) = \left(1 - \frac{\sigma(i,\, j,k+1/2)\delta t}{\varepsilon(i,\, j,k+1/2)}\right).E_z^n(i,\, j,k+1/2) + \frac{\delta t}{\varepsilon(i,\, j,k+1/2)\delta}\begin{bmatrix} H_y^{n+1/2}(i+1/2,\, j,k+1/2) - H_y^{n+1/2}(i-1/2,\, j,k+1/2) \\ + H_x^{n+1/2}(i,\, j-1/2,k+1/2) - H_x^{n+1/2}(i,\, j+1/.2,k+1/2) \end{bmatrix}, \tag{3.15f}$$

Fig. 3.2(a). Fig. 3.2(b) describes the quarter of a unit cell containing the all field components. when comprising boundary conditions it will be useful. In understanding the inflated system of Eqs. (3.15a)– (3.15f) into a code.

Accuracy and Stability

The spatial increase δ should be small and it should be relative to wavelength (typically ≤ λ/10) for the accuracy of results. This implies the unit wavelength having 10 or more cells. For the scheme of Eqs. (3.15a)– (3.15f), the time rise Δt should meet the stability condition [32, 36] given below:

$$u_{\max}\Delta t \le \left[\frac{1}{\Delta x^2} + \frac{1}{\Delta y^2} + \frac{1}{\Delta z^2}\right]^{-1/2} \tag{3.16}$$

where u_{max} denotes the maximum phase velocity of wave. Since we are using a three dimensional cell with Δx = Δy = Δz = δ, Eq. (3.16) becomes

$$\frac{u_{\max}\Delta t}{\delta} \le \frac{1}{\sqrt{n}} \tag{3.17}$$

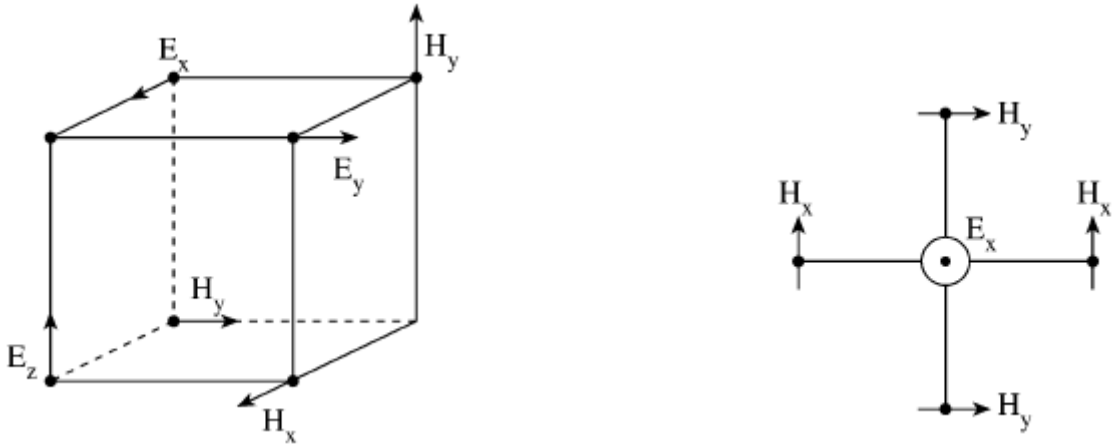

(a) (b)

Figure 3. 2 The relation between the field components: (a) with in the one fourth of the unit cell, (b) in a plane.

where space dimensions are denoted by n. The ratio of the rise in time to rise in spatial dimension has to be considered as large as possible for meeting Eq. (3.17) [37].

CHAPTER 4

ULTRA-WIDE BAND ANTENNAS

In this chapter, the design and analysis of simple compact lotus shaped planar monopole antennas and dual notch antenna are presented. The proposed antennas fabricated on a $44\times38\times1.58mm^3$ on a FR4 substrate. Simple antenna covers the frequency range from 2.86 to 14.0 GHz. The dual notch antenna covers the wide range 2.8 to 11 GHz with notch frequencies at 3.458 and 5.51GHz ranging from 3.35GHZ-3.566GHz and 5.285GHz-5.771GHz frequencies. The dual notch antenna can be used to avoid narrow band applications named as WiMAX and WLAN from UWB frequency range to avoid the interference.

Introduction

According to FCC [38] the UWB antenna should be operated in the range from 3.1 to 10.6 GHz bandwidth for commercial use. Micro strip antennas have narrow impedance bandwidth. To increase the impedance bandwidth so many techniques are implemented [39] among them some are directly coupled and gap coupled parasitic patches [40], implementation using U-slot patches [41] and E-shapes patches [42]. Using above techniques ten percent of bandwidth can be increased.

Different feed lines are used for investigating different types of UWB antennas like microstrip line [43]-[46], coplanar waveguide (CPW) [46] and various shapes like the crescent patch [44].

Some narrow band applications like WiMAX, WLAN etc. can cause interference to the UWB antenna system [47].

ANTENNA DESIGNS

Compact Lotus Shape Planar Monopole Antenna for UWB Applications

Geometry of proposed antenna

Fig. 4.1 shows the proposed antenna with its parameters. The proposed antenna radiator is combination of semicircular and triangular patch (lotus shape).

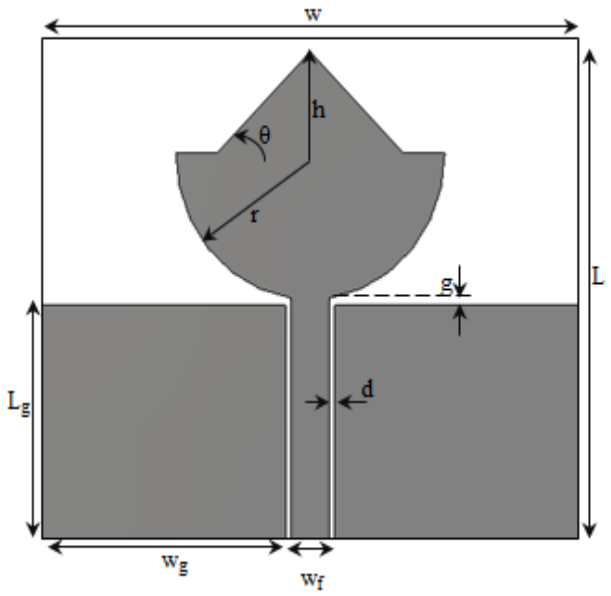

Figure 4. 1 Proposed geometry and its parameters

which is fed by 50 Ω CPW microstrip line. The antenna is oriented on a standard FR-4 substrate having a dielectric constant ε_r=4.4, loss tangent tan δ = 0.025 and thickness of 1.58mm.The dimensions of designed antenna are w=44 mm, L=38 mm, r=11 mm, θ=45°, h=7.6 mm, w_g=20 mm, L_g=17.6 mm, w_f=3.2 mm, g=0.6 mm, d=0.4 mm.

Simulation Results and Discussions

The simulation is performed using CST MW Studio 2012. The S11 of designed antenna is shown in Fig. 4.2. It is observed that the impedance bandwidth of 132.14 % from 2.86 to 14 GHz is achieved, which is suitable for UWB application. Fig. 4.3 depicts the S11 curves with various angles with other fixed parameters, the angle (θ) affects the resonance frequencies and the impedance bandwidth of antenna. It can be seen that the lower edges of the S!! curve moving

towards higher frequency and the impedance bandwidth decreases. Another observation is for radius (*r*) of lotus shape geometry. It can be seen from Fig. 4.4, when we increasing the '*r'*, it affects the resonance frequencies shifts towards the higher frequency as well as the impedance bandwidth of antenna not matching for UWB frequency range. At r=11 mm the impedance bandwidth is well matched below the -10 dB.

Fig. 4.5 depicts the radiation patterns of proposed lotus shape planar antenna at 3.4, 6.5 and 9.0 GHz. The patterns are Omnidirectional in nature for two principal planes (E- and H-plane). The antenna gain is plotted in Fig. 4.6. It is varied between 2.1 dB and 5.36 dB.

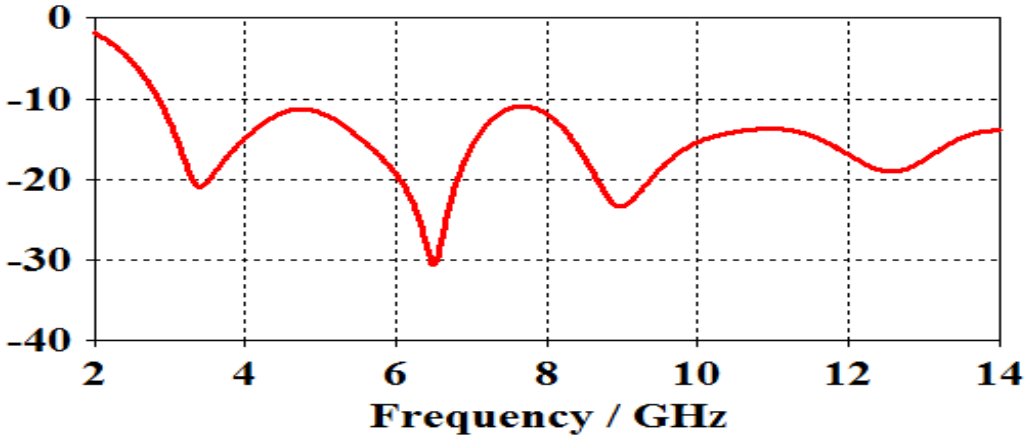

Figure 4. 2 Simulated S11 curve of proposed UWB antenna

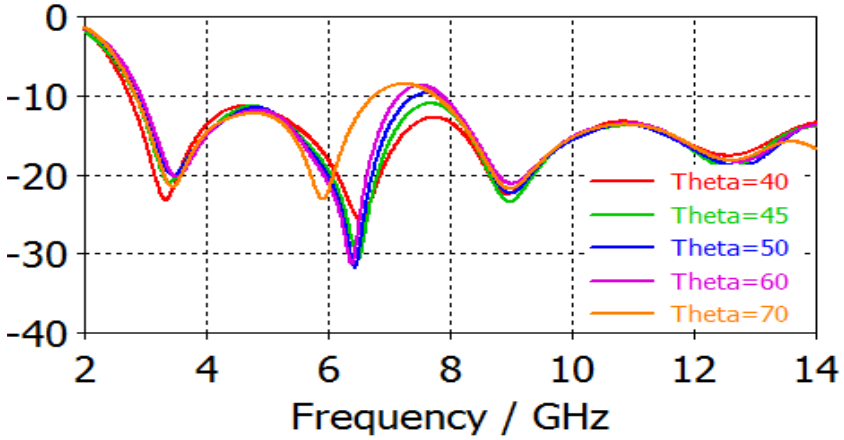

Figure 4. 3 Simulated S11 curve of different angles (theta) proposed UWB antenna

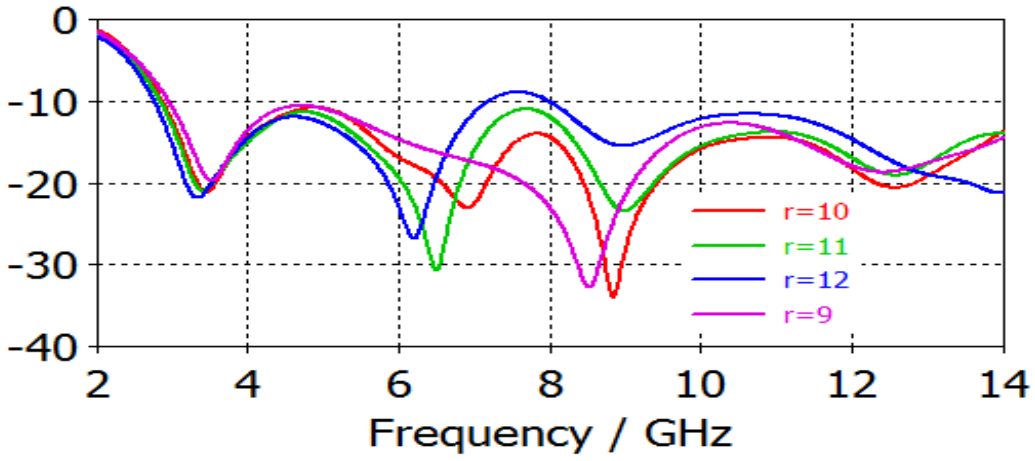

Figure 4. 4 Simulated S11 curve of different radii for proposed UWB antenna

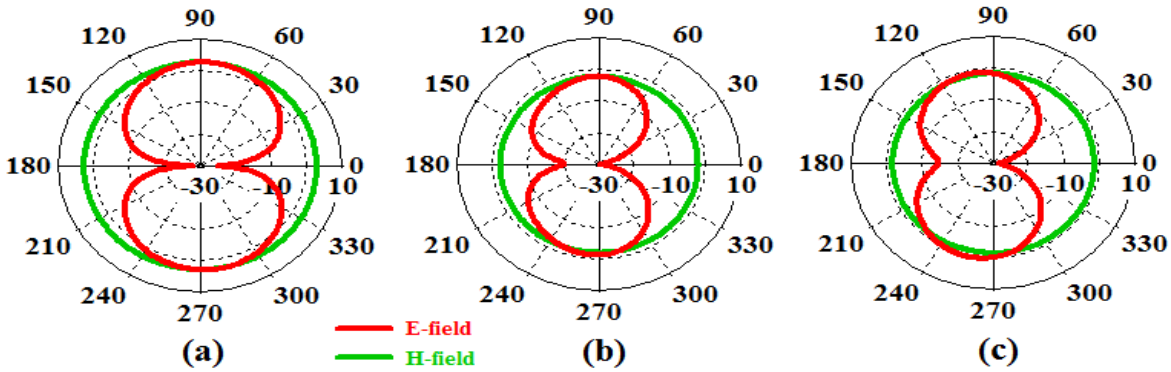

Figure 4. 5 Simulated radiation patterns of designed UWB antenna at (a)3.4 GHz (b) 6.5GHz (c)9 GHz

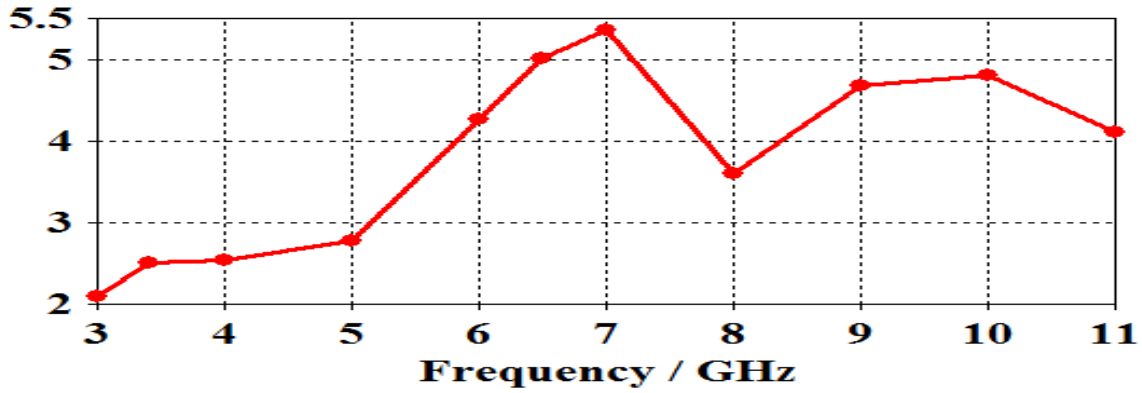

Figure 4. 6 Simulated gain vs. frequency curve of proposed UWB antenna

Compact Lotus Shape Planar dual notch Monopole Patch Antenna

Geometry of proposed antenna

Two notches have added for the previous geometry at the frequencies 3.458GHz and 5.51GHz frequencies for notching WiMAX and WLAN applications. Here two slots are inserted to achieve the two notch frequencies. The length of the slots are about half of the wavelength of the notch frequencies. In the slot at the front side, the angle θ is varying to control the centre frequency of the notch band and for the slot at the rear view is controlled by width of slot paramter.The dimension θ considered is 91°. The proposed antenna geometry is shown in Fig.4.7

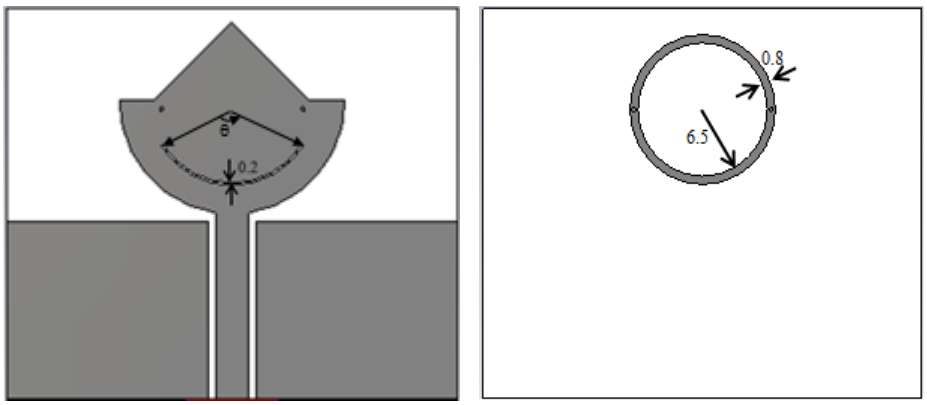

a) Front view b) back view

Figure 4. 7 Geometry and design parameters of proposed antenna

Simulation Results and Discussions

The simulation is performed using CST MW Studio 2012. The S11 of designed antenna is shown in Fig. 4.8. It is observed that there are two notch bands at frequencies at 3.458GHz which is for WiMax and 5.51GHz which is for WLAN Fig. 4.9 and Fig. 4.10 depicts the surface current distribution at two notch frequencies at 3.458GHz and 5.51GHz.

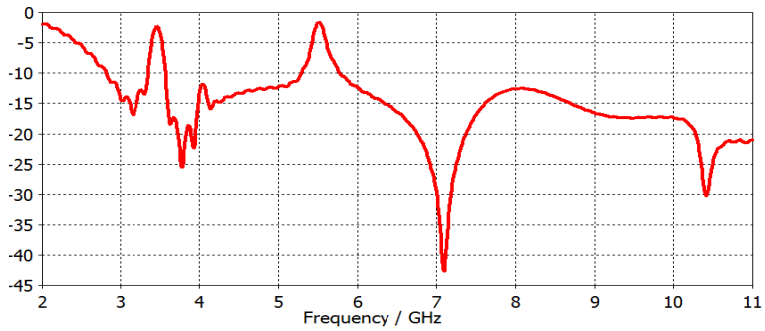

Figure 4. 8 Simulated S11 curve of proposed antenna

It is observed that at these resonant frequencies maximum of the current is situated at respective slots. It can be seen from Fig. 4.11, the VSWR for designed antenna is below two, except at notch frequencies where the VSWR is 7.16 and10.689 at 3.458GHz and 5.51GHz respectively. The antenna gain is plotted in Fig. 4.12. It is varied between 2.1 dB and 5.36 dB.

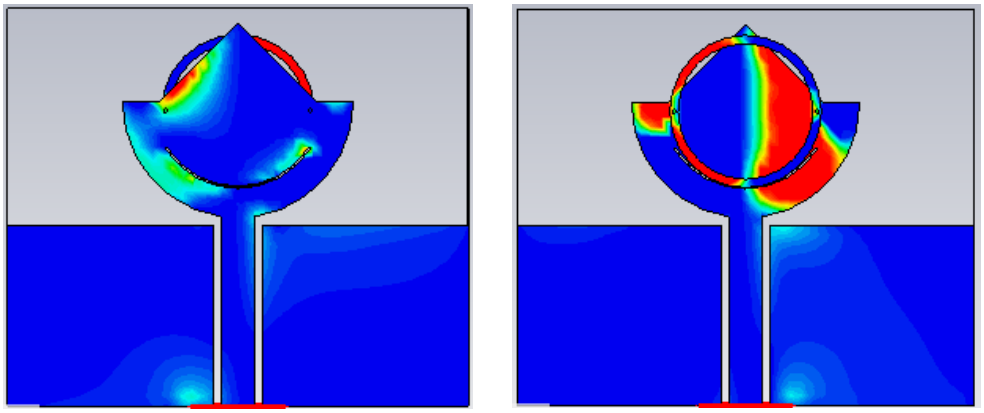

Figure 4. 9 Surface current distribution at 3.458GHz of the designed antenna

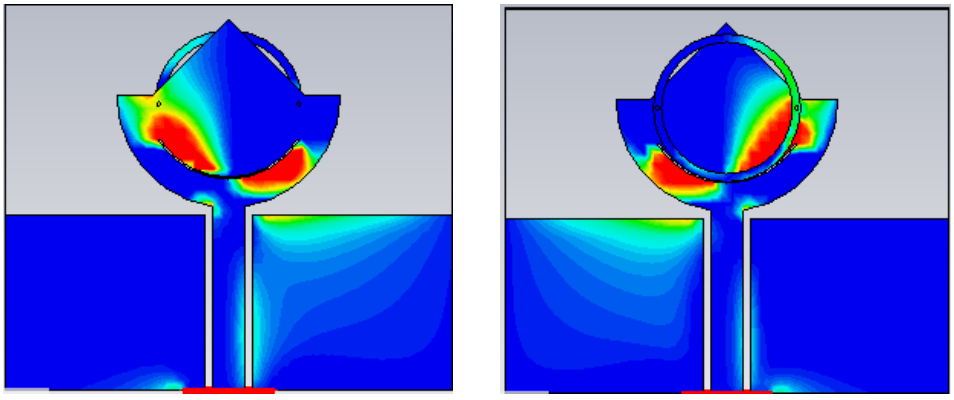

Figure 4. 10 Surface current distribution at 5.51GHz of the designed antenna

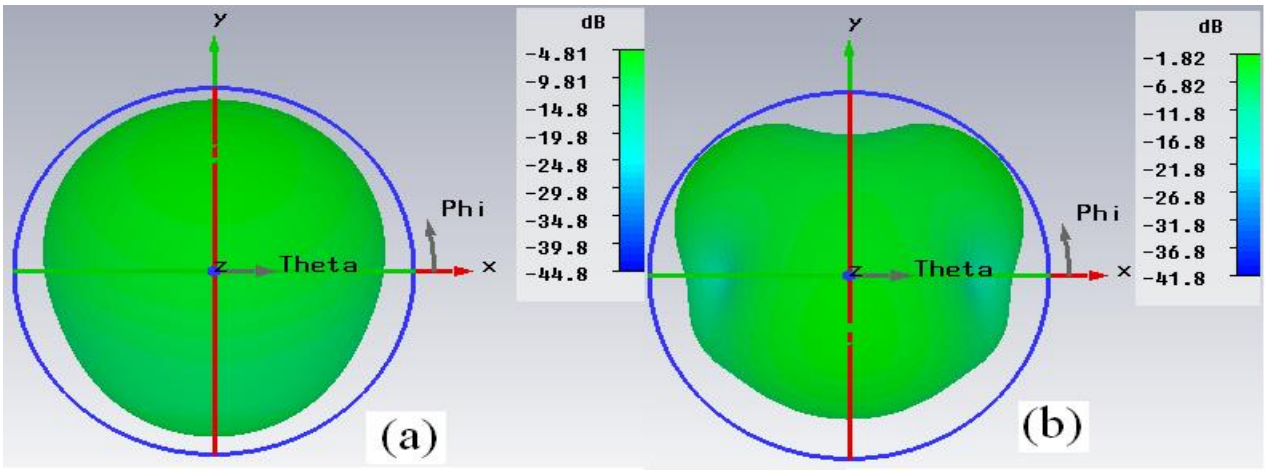

Figure 4. 11 Simulated 3D radiation pattern of the designed antenna at (a) 3.458GHz (b) 5.1GHz

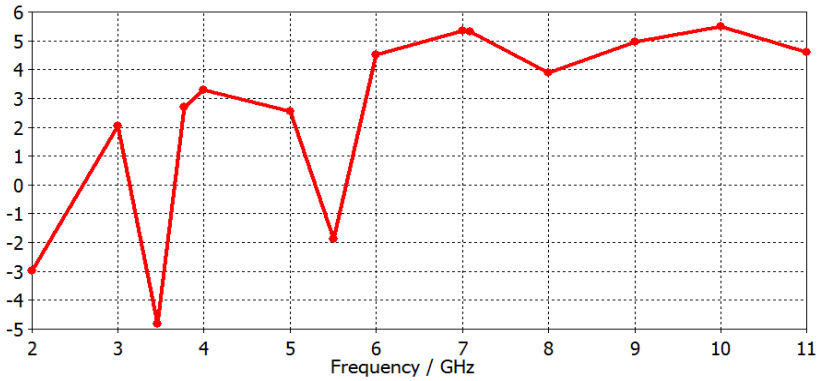

Figure 4. 12 Simulated gain vs. frequency curve of the proposed antenna

CHAPTER 5

TWO ELEMENT UWB MIMO ANTENNAS

MIMO

In modern era of wireless communications MULTIPLE-INPUT-MULTIPLE-OUTPUT (MIMO) technology gains an attracted attention. By deploying multiple antennas for transmission an array gain and diversity gain can be accomplished therefore, the spectral efficiency and reliability of is increased significantly and an increase in channel capacity without costing the additional bandwidth or transmit power. MIMO antenna systems require high isolation between antenna ports and a compact size for applications in portable devices.

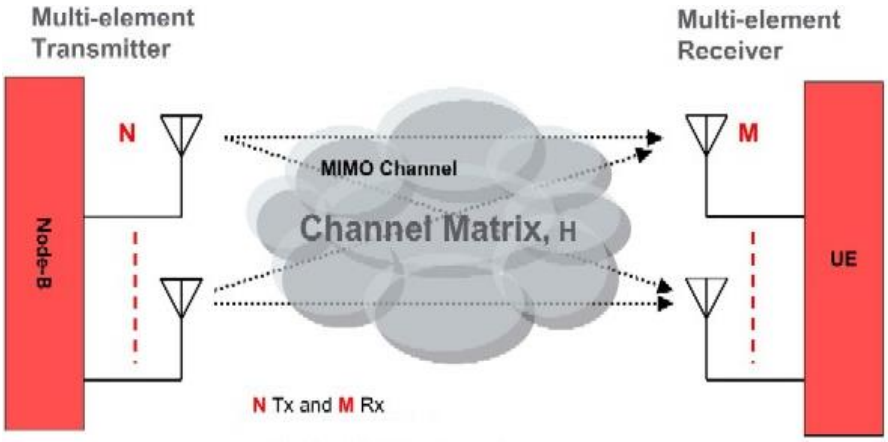

Figure 5. 1 MIMO system

Multiple antennas are used at the both transmitter and receiver section in MIMO technique. It can combine both the SIMO and MISO technologies and by using Spatial Multiplexing (SM) technique can also increase capacity. By comparing the MIMO with the Single-input Single-output (SISO) methods, MIMO has various advantages. In MIMO spatial diversity is used to avoid the fading and it requires low power.

Ultra-wideband MIMO Antennas

Recently, there is a demand in increasing the data rate of existing wireless communication systems. By assuming typically two antennas in a mobile terminal the data rate and reliability can be enhanced by employing the diversity techniques without sacrificing

additional spectrum or transmitted power in rich scattering environments. The channel capacity can further increased by MIMO UWB systems related to normal MIMO systems. However, for a MIMO antenna to be implemented in a multifunctional portable device, the following challenges are to be considered during the design of these antennas.

Design Challenges in UWB MIMO antenna systems

- **Isolation:** While designing MIMO systems there are need to concern about mutual coupling between antennas. Because it will influence the both antenna efficiency as well as the correlation. Isolation better than -16 dB is to be accomplished throughout the operating region of the antenna system.
- **Bandwidth:** Return loss (S11 in dB) should be less than -10 dB from 3.1 to 10.6 GHz so that the impedance bandwidth covers the entire UWB. To enhance the both isolation and impedance bandwidth in a single antenna structure is biggest challenge that exists in the design of a UWB MIMO antenna system.
- **Size:** Various communication technologies such as WCDMA, WiMAX, WLAN, and UWB have been adapted in mobile phones in order to realize high speed data transmission. Evidently, such applications require a compact wide-band MIMO antenna because of the limited space available in wireless devices.

Hence the UWB MIMO antenna systems which are having small in size and reduced mutual coupling are desired for UWB applications.

Isolation and Bandwidth Enhancement:

To enhance the both bandwidth and isolation simultaneously numerous methods and isolation structures have been introduced in a UWB MIMO antenna system.

By introducing reflectors in a ground plane and stubs in some designs the mutual coupling can be reduced. Slots can be inserted in the patch for increasing the bandwidth. Several studies have been carried out on various MIMO antenna systems with two and four radiating elements and various methods have been proposed to improve isolation between the antennas. Various structures like mushroom–shaped EBG structures have been proposed to reduce mutual coupling by inhibiting the current running between the radiating patches. Low mutual coupling can also be accomplished through neutralization techniques and decoupling networks.

Anechoic Chamber

Anechoic Chamber is an antenna measurement chamber. It is a closed room consisting pyramidal-like arrangement on the side walls with conical shape facing outside the wall. All the walls of the room are coated with metals. This is done to avoid the radiation effect on the measurement of the test antenna from outside environment. The pyramidal like dome shape is made to make the characteristic impedance of atmosphere to match with the characteristic impedance of the Antenna under Test (AUT).

Chamber is having a positioner to fix the test antenna and the reference antenna is kept at other end having same polarization as that of the test antenna. The anechoic chamber and its flowchart shown in Fig. 5.2 and Fig.5.3 describes the measurement operation to be done to test the characteristics of the antenna. The directional coupler is fed by source power which is distributed to amplifier and mixer. The reference antenna is fed by amplified power received by the receiver. This power will be radiated in the atmosphere inside the chamber and received by the AUT. The power received by mixer from the directional coupler and AUT are compared to the Local Oscillator (LO) frequency to produce same Intermediate Frequency (IF) that is received by the receiver Rx. The positioner is connected to the positional controller that will control the axis and position of the AUT and a system (Computer) is linked to it to calculate the various results at different desired axis and position of the AUT.

There is basically four axis control system used for measurement. They are Azimuthal, Slide Roll and Elevation axis control system. Out of these, the first three control systems are used for main measurement and the last one is used for phase measurement.

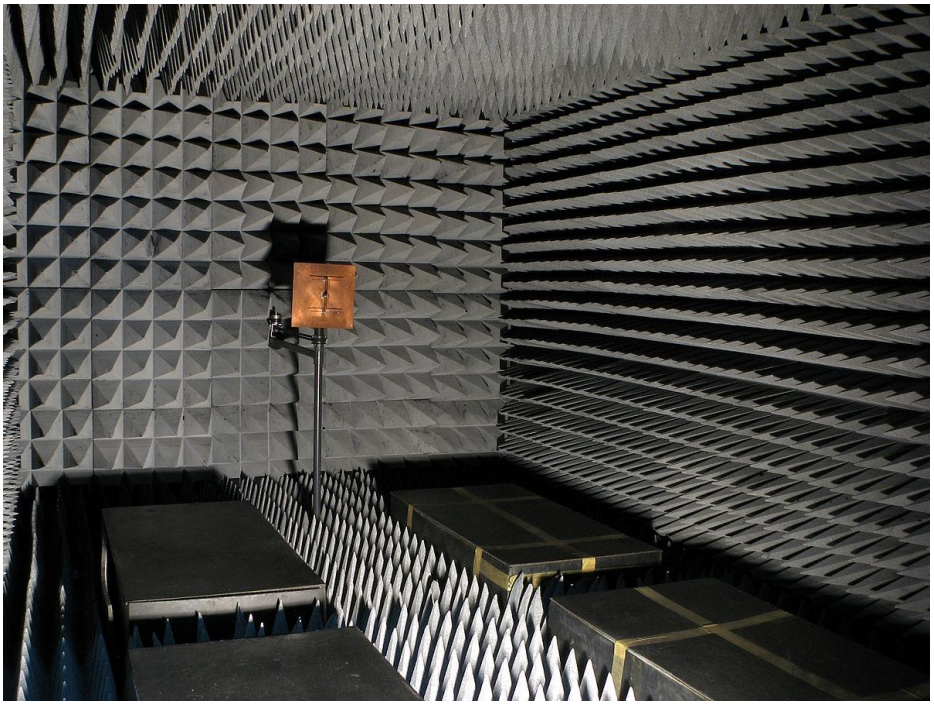

Figure 5. 2 Anechoic chamber

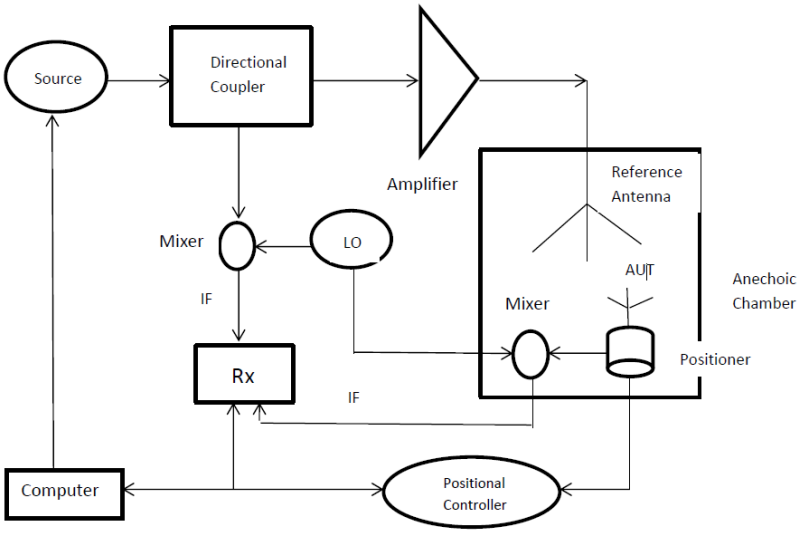

AUT- Antenna Under Test

IF- Intermediate Frequency

Figure 5. 3 Anechoic Chamber Operation flowchart

Two element compact UWB MIMO Antenna systems

A Compact Lotus Shape Planar Antennas System for UWB-MIMO Applications

Geometry of proposed antennas

The proposed antenna systems having two identical lotus shaped antenna elements instanced in Fig. 5.4. Here three different are proposed by considering the first design exemplified in previous

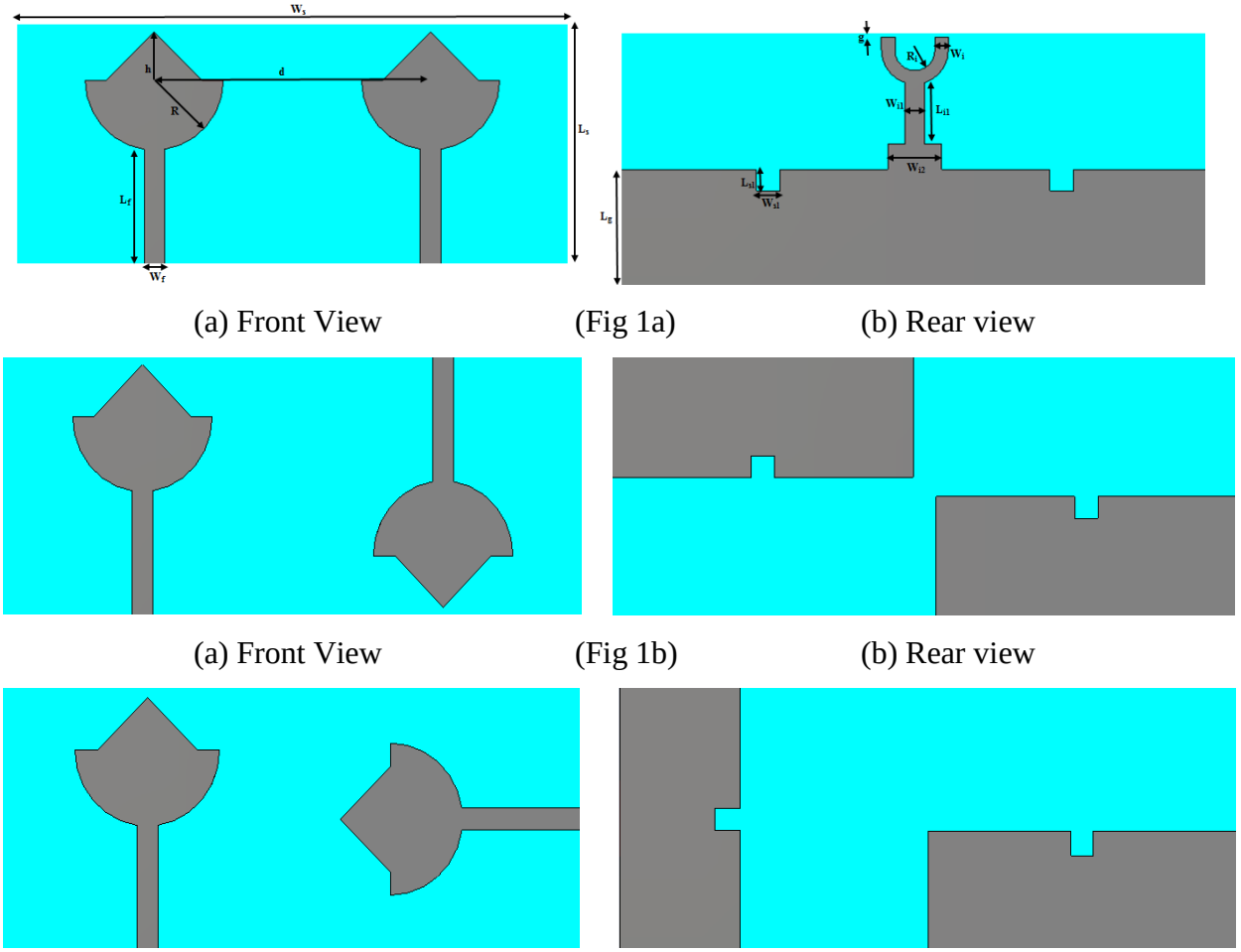

Figure 5. 4 Geometry and design parameters of the proposed antennas

chapter i.e. compact lotus shaped planar antenna. The antenna element is fed by standard 50Ω microstrip line presented by choi et al [48]. The antenna system is oriented on an FR4 substrate having a dielectric constant ε_r=4.4 and 1.6mm thickness. The dimensions of the designed antenna

system shown in fig.1a are W_s=88mm, L_s=38mm, h=7.6mm, r=11mm, L_f=18.4mm, L_g=17.6mm, R_i=3mm, W_i=2mm, W_{i1}=3mm, L_{i1}=9.3mm, W_{i2}=8mm, L_{s1}=3.2mm, W_{s1}=3.6mm,

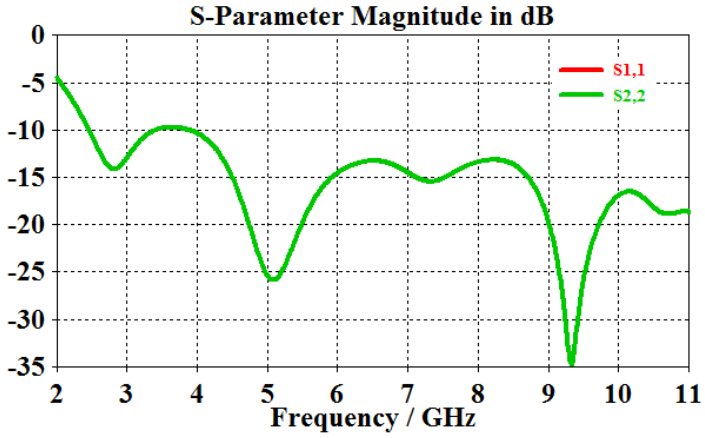

(a)

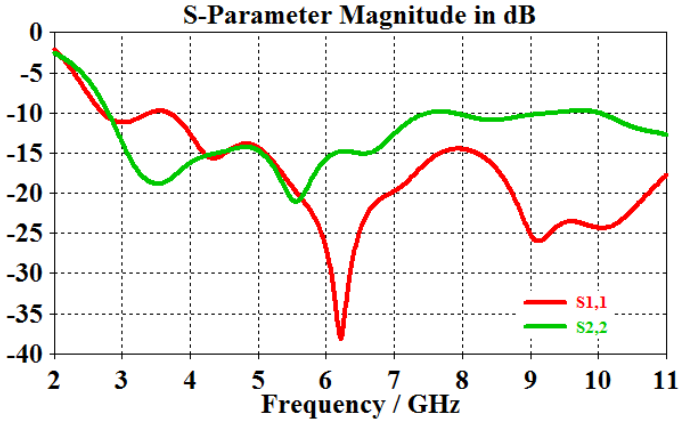

(b)

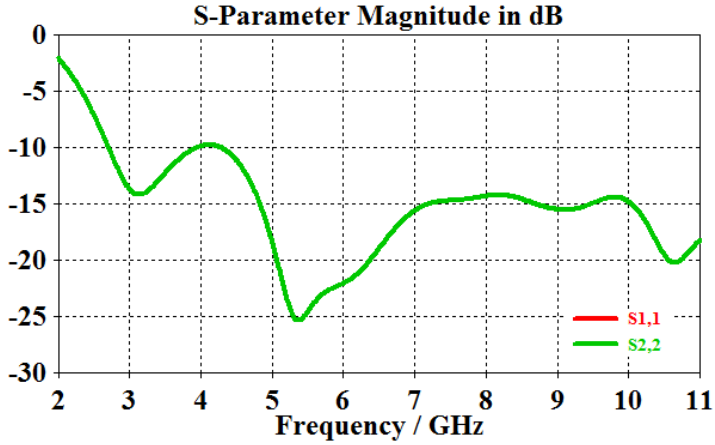

(c)

Figure 5. 5 Simulated S11 curves for the antennas placed (a) 0 degrees (b) 90 degrees (c) 180 degrees on a substrate.

g=0.5mm, d=44mm. Planar antenna system is designed with reduced mutual coupling for efficient radiation. In the proposed system the lotus shaped antennas are placed in three different angular positions i.e. 0, 90,180 degrees. These are simulated to observe the S11 pattern and mutual coupling between them.

Simulation results and discussions

Return Loss:

The simulation is performed using CST MW Studio 2012. The S11 curves for the proposed three antenna systems are shown in Fig. 5.5. The results indicate that the S11 is less than -10 dB over the desired range of frequencies. The curves of S11 and S22 are identical to each other because of the reciprocity and the similar is with S12 and S21 for the antennas placed in parallel and 180 degrees respectively. But when the antennas are placed 90 degrees on the substrate the S11 and S21 are different because, with respect to length and width, the two patch antennas are having different dimensions of the substrate. Among three the antenna system consisting the elements placed on parallel on the substrate is fabricated and measured. The evaluated results are well matched to the theoretical results. The prototype of antenna and compared result of S-parameter is shown in Fig. 5.6 and Fig. 5.7.

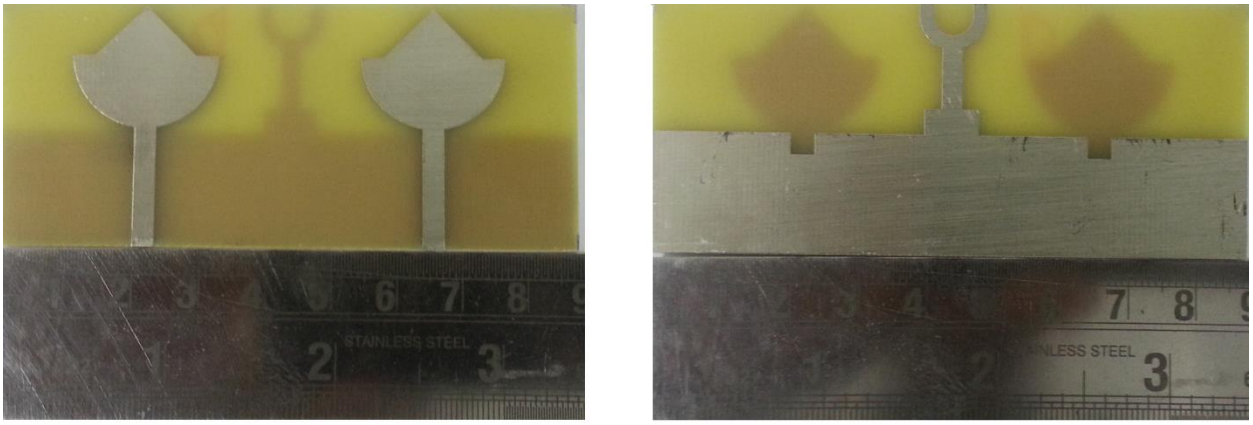

(a) (b)

Figure 5. 6 prototype of the designed antenna

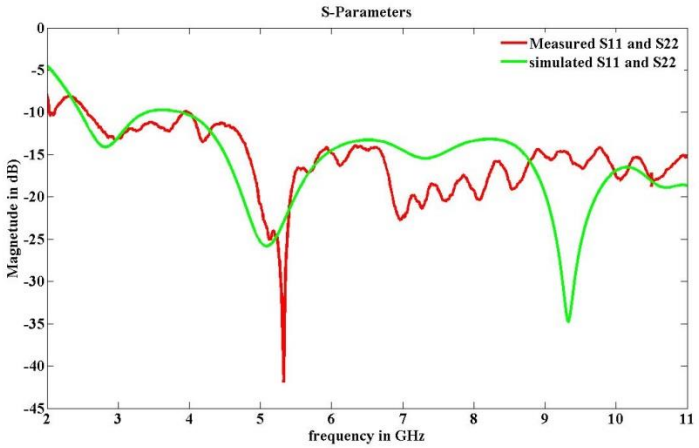

Figure 5. 7 Simulated and measured S-Parameter curve for the fabricated antenna.

Mutual coupling:

The designed single antennas as mentioned in chapter 4 are placed in three different angular positions to each other to get the maximum isolation between them. The mutual coupling is best candidate to judge the performance of antenna system for UWB MIMO system. The fork shape design is used for providing isolation. The mutual coupling is evaluated by conceiving the excitation of one antenna and matching the other antenna with 50 Ω impedance is shown in Fig.5.8. From the results it is observed that mutual coupling (S21 or S12) is always than -15 dB in the concern frequency range.

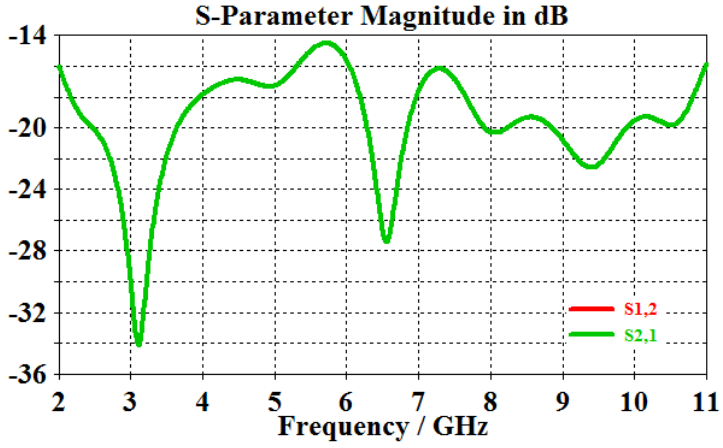

(a)

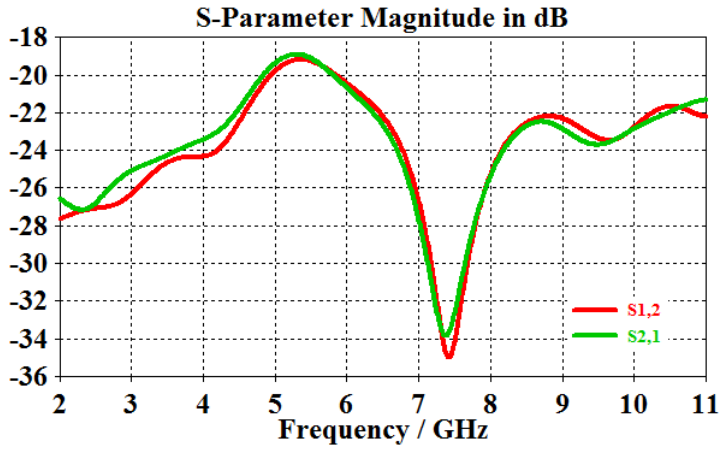

(b)

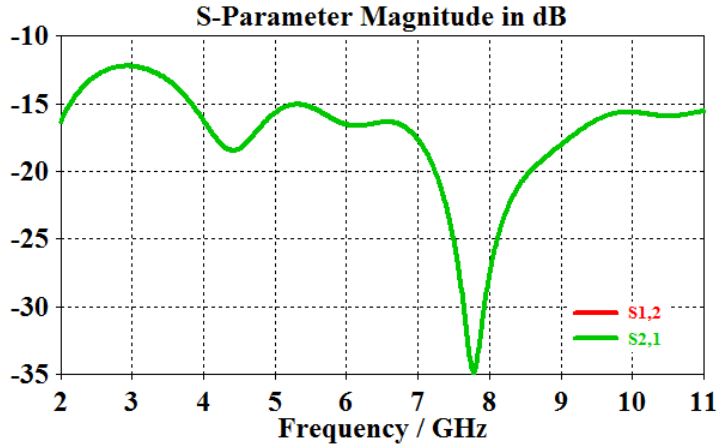

(c)

Figure 5. 8 Mutual coupling between the antennas placed (a) 0 degrees (b) 90 degrees (c) 180 degrees on a substrate

However, there is better isolation between the antennas when the antennas are placed orthogonal to each other relative to other positions. The measured results are well matched to the simulated mutual coupling for the antenna system consisting the elements placed on parallel on the substrate is shown in Fig 5.9.

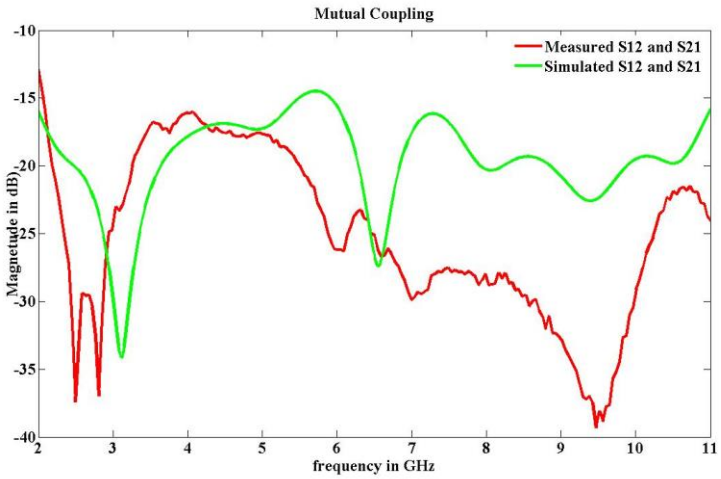

Figure 5. 9 Simulated and measured Mutual coupling between the antennas for fabricated antenna.

Radiation patterns and gain:

The designed antennas system are in X-Y plane. The polar radiation patterns for the frequencies 4 GHz, 6 GHz and 8 GHz in X-Y plane for proposed antenna system are presented in Fig.10. The gain of antenna is plotted in Fig. 11. The maximum realized gain achieved is 5.95 dB when the antennas are placed parallel to each other.

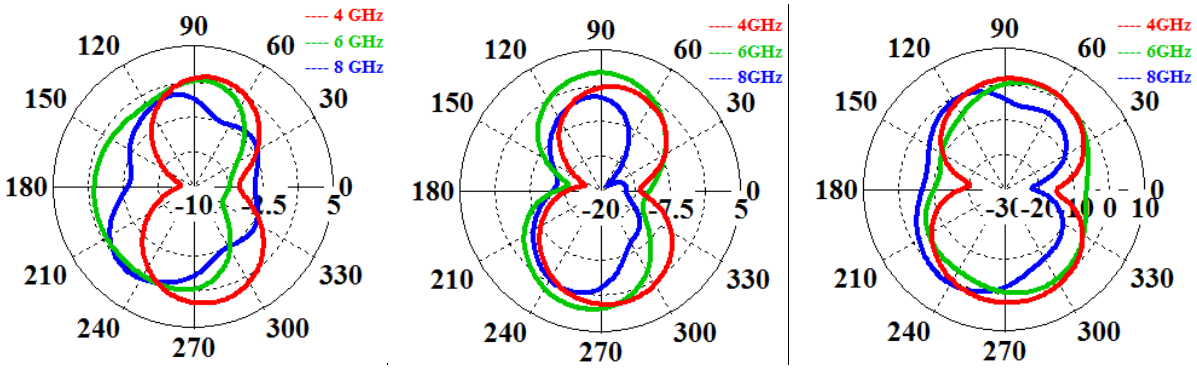

(a) **(b)** **(c)**

Figure 5. 10 Radiation patterns of antennas placed (a) 0 degrees (b) 90 degrees (c) 180 degrees on a substrate

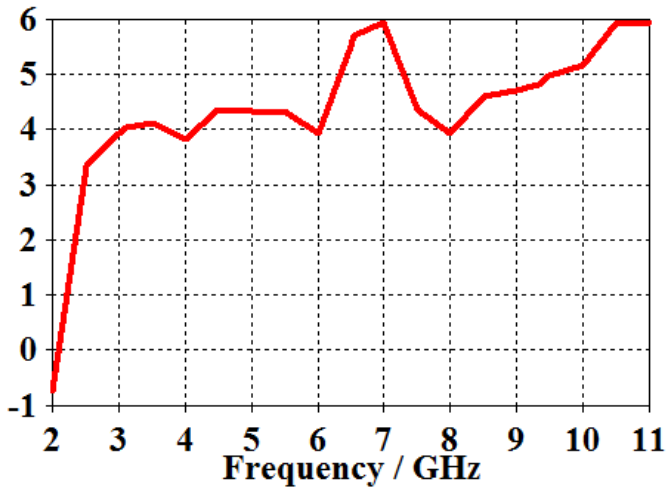

(a)

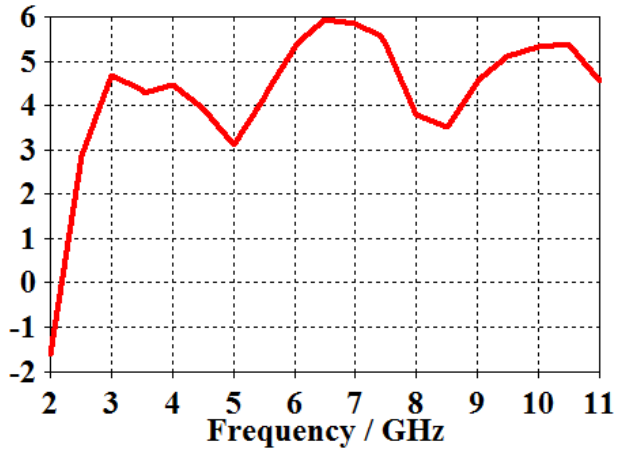

(b)

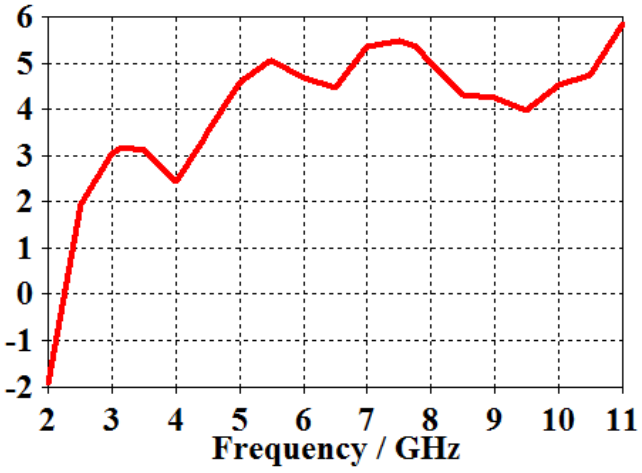

(c)

Figure 5. 11 Simulated gain vs. frequency curve of antennas placed (a) 0 degrees (b) 90 degrees (c) 180 degrees on a substrate

Total active reflection coefficient (TARC):

The TARC is similar to S11 and having the range from Zero to one. But S11 Considers single antenna. TARC considers complete array as one element. Here, the accepted power is directly relates to its input power of a multiport antenna. For evaluating TARC mutual coupling is considered [49].

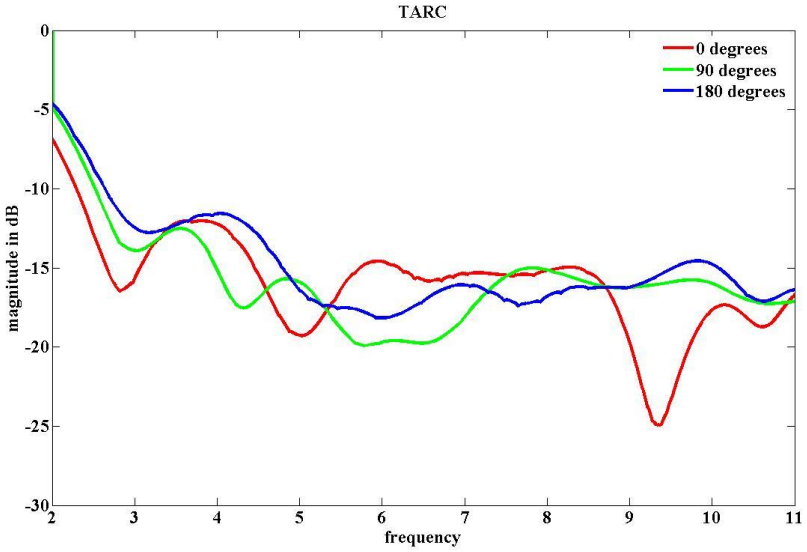

Figure 5. 12 Calculated Total active reflection coefficient (TARC) for three antenna systems

The TARC can be calculated as follows [50]

$$TARC = \frac{\sqrt{\left|S_{11} + S_{12}e^{j\theta}\right|^2 + \left|S_{21} + S_{22}e^{j\theta}\right|^2}}{\sqrt{2}},$$

Where S11, S12, S21 and S22 are elements of S matrix, and θ is the excitation frequency in different phases. The plot is shown in Fig. 5.12 and here, this parameter is evaluated for by considering 21 excitations with equidistant θ phases from 0 to 2π.

Envelope Correlation and Capacity loss:

The envelope correlation is an important parameter to evaluate the diversity capabilities for MIMO applications. The envelope correlation ρ_e is obtained from the correlation coefficients as

$$\rho_e(i, j, N = 2) = \frac{\left|\rho_{ij}\right|^2}{\rho_{ii}.\rho_{jj}}.$$

The correlation coefficients are then given by [51, 52]

$$\rho_{ii} = 1 - \left(\left| S_{ii} \right|^2 + \left| S_{ij} \right|^2 \right),$$

$$\rho_{ij} = -\left(S_{ii}^{*} S_{ij} + S_{ji}^{*} S_{jj} \right).$$

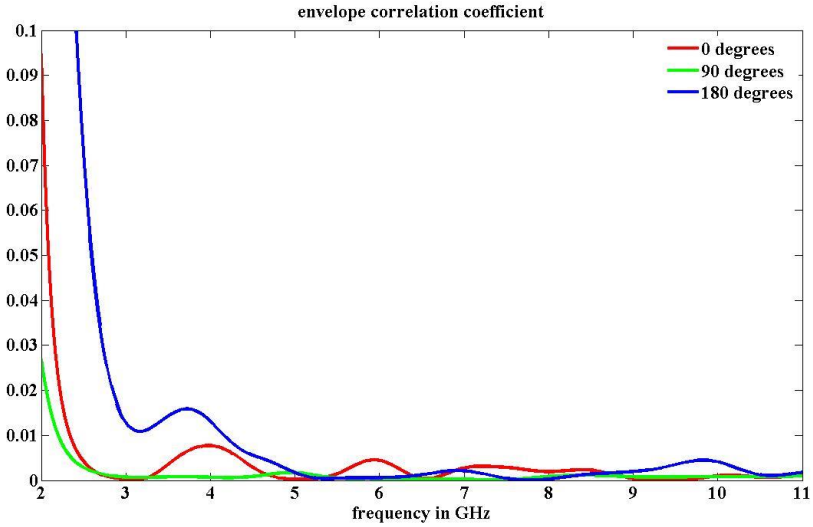

Figure 5. 13 Calculated envelope correlation coefficient for three antenna systems

Fig. 5.13 shows the envelope correlation plot over the frequency range. Typically, it is considered that antennas with less than 0.7 correlation are capable for good diversity performance [53]. From the Fig.13 it is observed that the system having less correlation when the antennas are placed orthogonal to each other and the coefficient is less than 0.03 is achieved. But, when the antennas are placed 180 degrees on the substrate the achieved coefficient is less than 0.5 which is quite high compared to orthogonal system. As number of antennas increased the capacity also increases. A loss of capacity is induced by the correlation between the antennas. For high SNR, capacity loss is given by [55],

$$C_{loss} = -\log_2 \det\left(\Psi^R\right)$$

Where Ψ^R is the receiving correlation matrix

$$\Psi^R = \begin{pmatrix} \rho_{11} & \rho_{12} \\ \rho_{21} & \rho_{22} \end{pmatrix}.$$

The elements ρij stands for correlation coefficients. The reflections affect C_{loss}. So, by considering the TARC in to account in the calculation of capacity loss accurate results can be obtained. Then the true loss is given by

$$C_{total\_loss} = -2\log_2(1 - TARC^2) - \log_2 \det(\Psi^R).$$

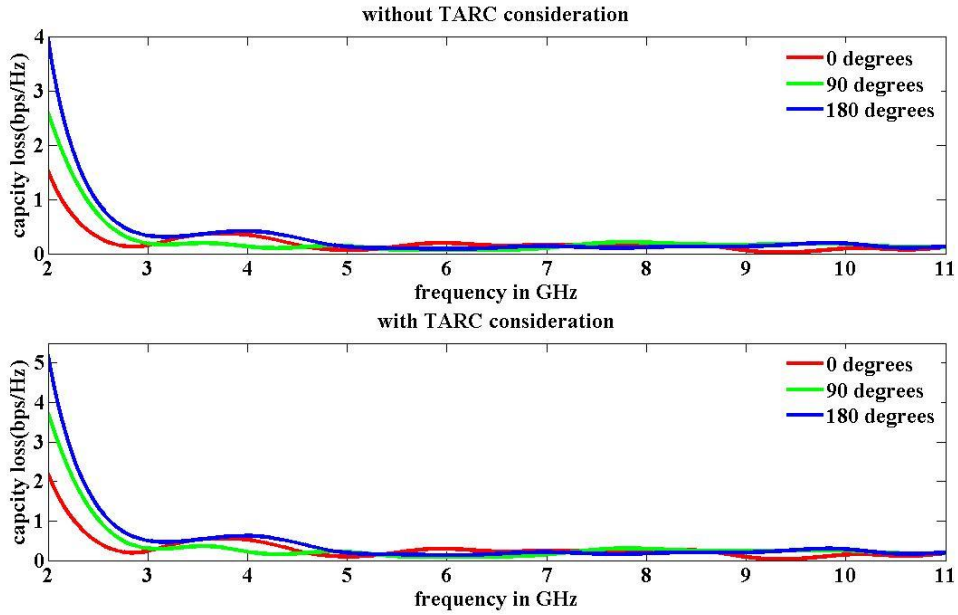

Figure 5. 14 Calculated Capacity Loss for three antenna systems

Fig. 5.14 shows the capacity loss considering with and without TARC for the proposed antenna system. As shown in Fig. 5.13, the lowest correlation causes the lowest capacity loss. From the Fig. 5.14 it is observed that capacity loss increases as we move from 0 degrees to 180 degrees and the lowest capacity loss achieved is below 2 bps/Hz when the antennas are placed parallel to each other.

A Compact Dual Notch Lotus Shape Planar Antennas System for UWB-MIMO Applications

Geometry of proposed antennas

The proposed antenna systems having two identical dual notch lotus shaped antenna elements instanced in Fig. 5.15. Here three different structure are proposed by considering the second design exemplified in previous chapter i.e. compact lotus shaped planar antenna. The dual notch lotus

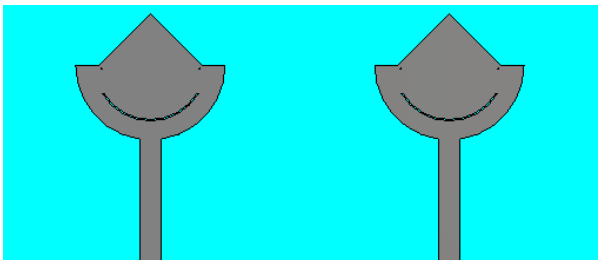

(a) Front View (Fig 1a) (b) Rear view

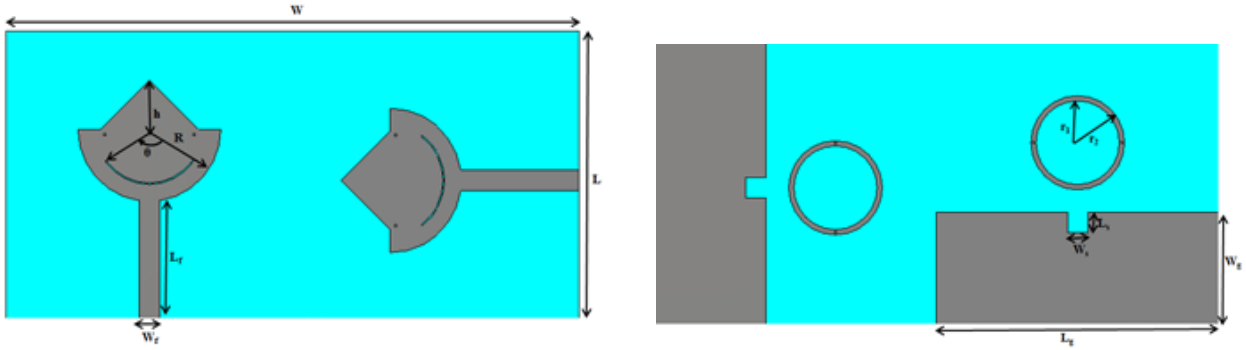

(a) Front View (Fig 1b) (b) Rear view

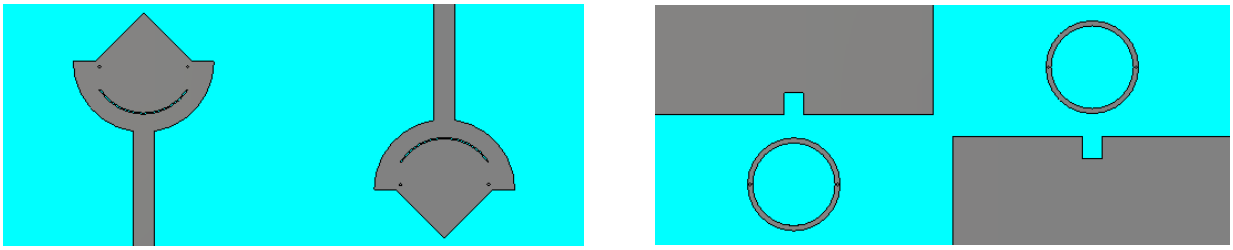

(a) Front View (Fig 1c) (b) Rear view

Figure 5. 15 Geometry and design parameters of the proposed antennas

shaped patch element is standard 50Ω microstrip line presented by choi et al [48]. The antenna system is oriented on an FR4 substrate having a dielectric constant ε_r=4.4 and 1.6mm thickness. The dimensions of the proposed antenna system shown Fig.1b are L=44mm, W=88mm, h=7.6mm, R=11mm, L_f=18.2mm, w_f=3.2mm, θ=91˚, r_1=6.5mm, r_2=7.3mm, L_g=44mm, w_g=17.4mm, L_s=3.2mm, W_s=3.2mm. Planar antenna system is designed with reduced mutual coupling for efficient radiation. In the proposed system the lotus shaped antennas are placed in three different angular positions i.e. 0, 90,180 degrees. These are simulated to observe the S11 pattern and mutual coupling between them.

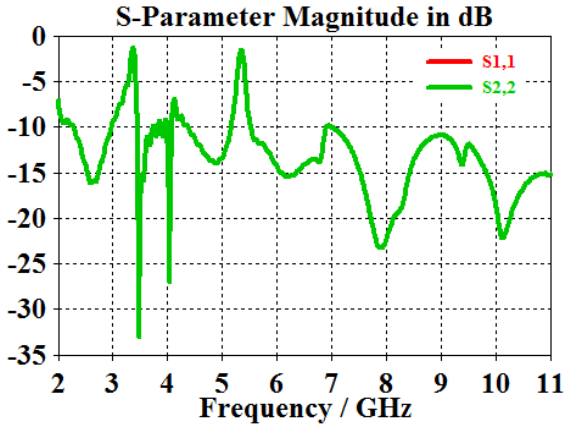

(a)

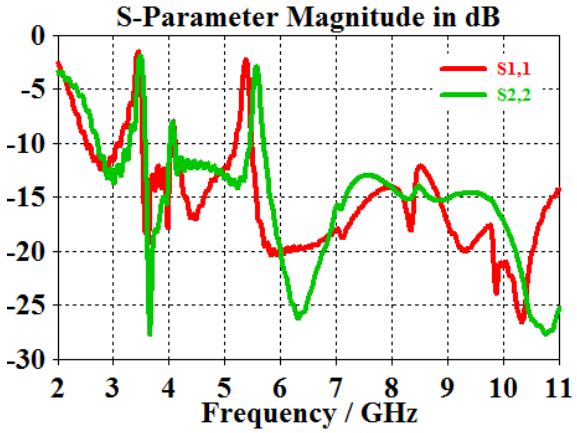

(b)

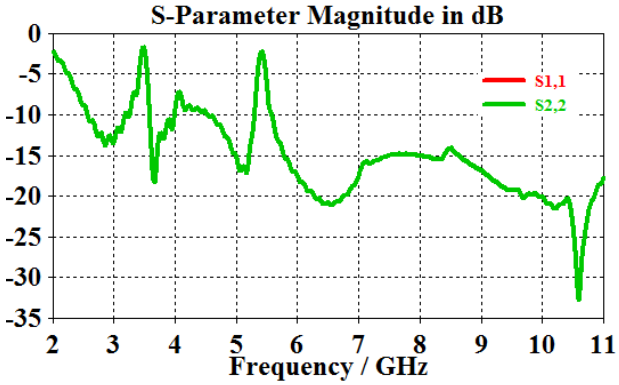

(c)

Figure 5. 16 Simulated return loss curves for the antennas placed (a) 0 degrees (b) 90 degrees (c) 180 degrees on a substrate

Simulation results and discussions

Return Loss:

The simulation is performed using CST MW Studio 2012. The return loss curves for the proposed three antenna systems are shown in Fig. 5.16. The results indicate that the S11 < -10 dB over the frequency range except notch frequency ranges. The curves of S11 and S22 are identical to each other because of the reciprocity and similar with S12 and S21 for the antennas placed in parallel and 180 degrees respectively. But when the antennas are placed 90 degrees on the substrate the S11 and S21 are different because, with respect to length and width, the two patch antennas are having different dimensions of the substrate. Among three the antenna system consisting the elements placed on parallel on the substrate is fabricated and measured. The measured results are well matched to the simulated results. The prototype of antenna and compared result of S-parameter is shown in Fig. 5.17 and Fig. 5.18.

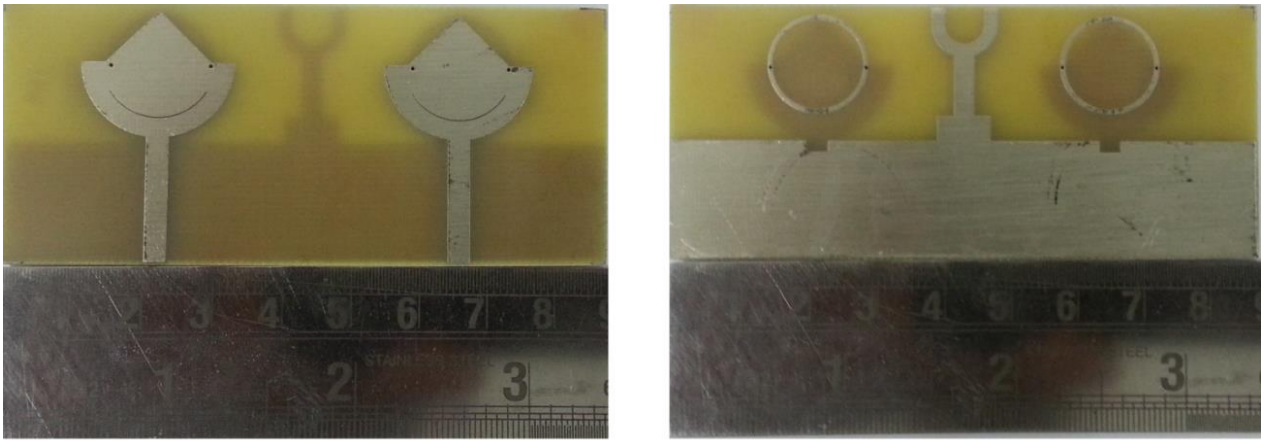

(a) (b)

Figure 5. 17 The prototype of the proposed antenna

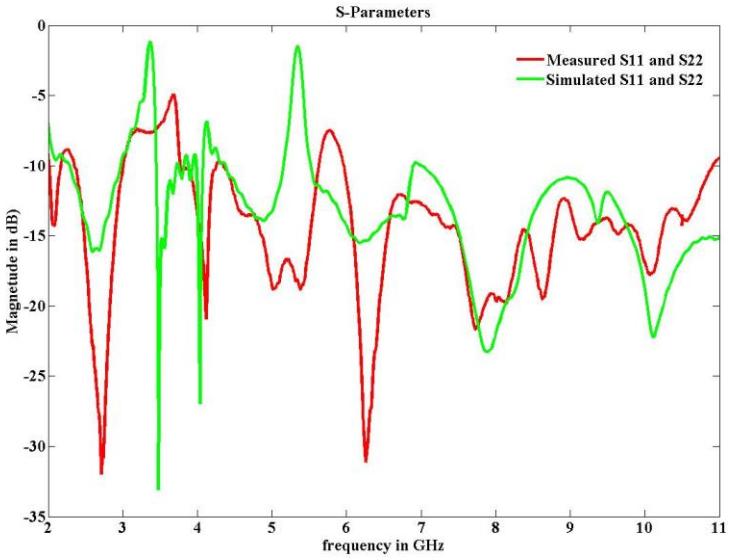

Figure 5. 18 Simulated and measured S-Parameter curve for the antennas placed parallel on the substrate

Mutual coupling:

The designed single antennas as mentioned in chapter 4 are placed in three different angular positions to each other to get the maximum isolation between them. The mutual coupling is best candidate to judge the performance of antenna system for UWB MIMO system. The fork shape design is used for providing isolation. The mutual coupling is evaluated by conceiving excitation of one antenna and matching the other antenna with 50 Ω impedance is shown in Fig. 5.19. From the results it is observed that mutual coupling (S21 or S12) is always than -15 dB in the concern frequency range. However, there is better isolation between the antennas when the antennas are placed orthogonal to each other relative to other positions. The measured results are well matched to the simulated mutual coupling for the antenna system consisting the elements placed on parallel on the substrate is shown in Fig. 5.20.

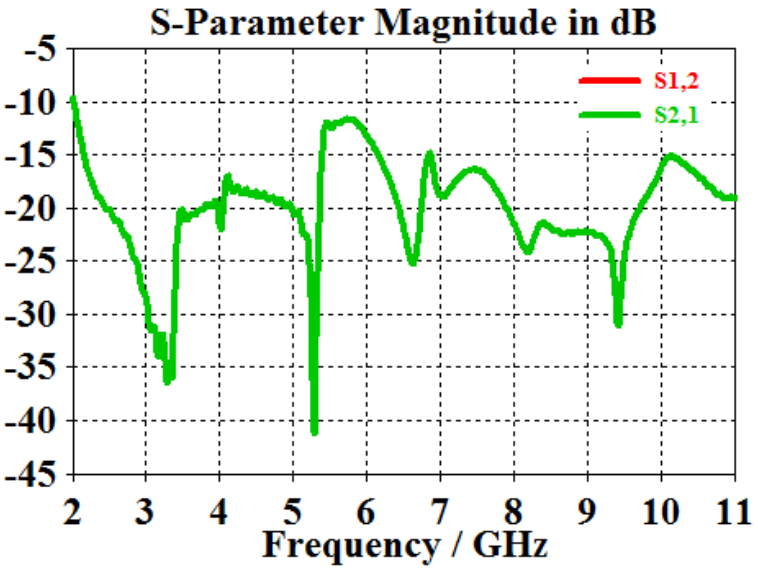

(a)

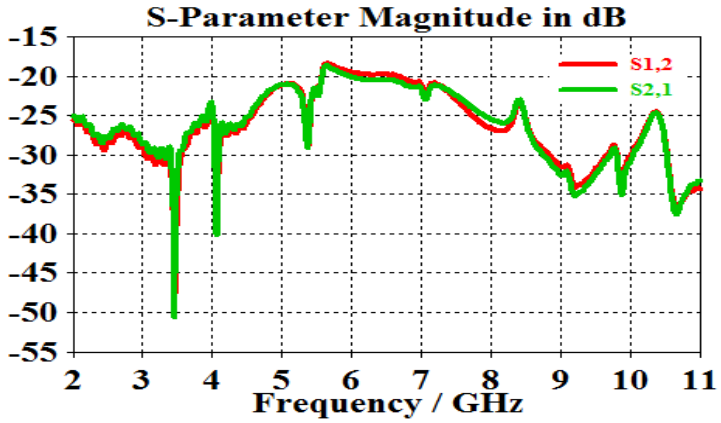

(b)

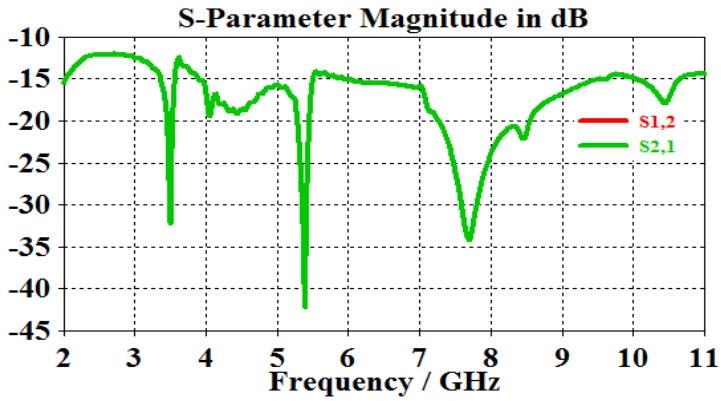

(c)

Figure 5. 19 Mutual coupling between the antennas placed (a) 0 degrees (b) 90 degrees (c) 180 degrees on a substrate

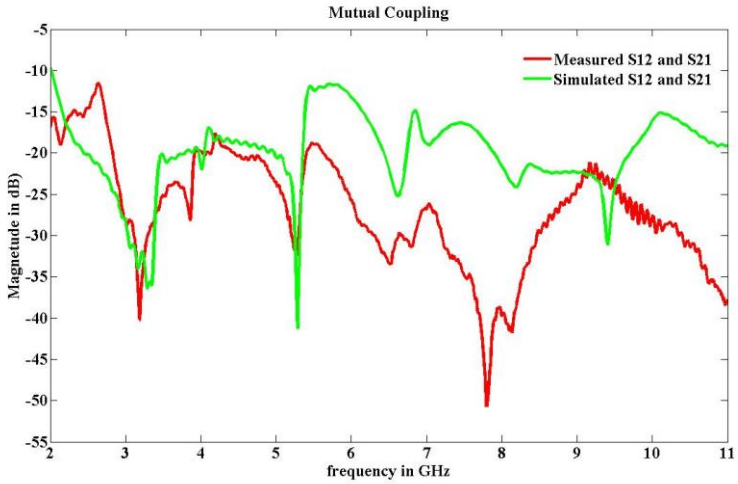

Figure 5. 20 Simulated and measured Mutual coupling between the antennas for fabricated antenna.

Radiation patterns, current distribution and gain:

The designed antennas systems are in X-Y plane. The polar radiation patterns for the frequencies 4 GHz, 6 GHz and 8 GHz in X-Y plane for proposed antenna system are presented in Fig. 5.21. The gain of antenna is plotted in Fig. 5.22. The maximum realized gain

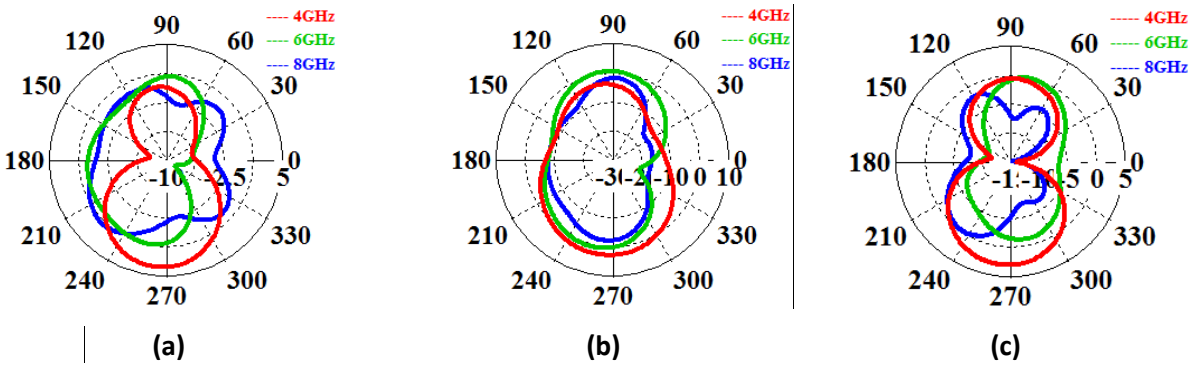

Figure 5. 21 Radiation patterns of antennas placed (a) 0 degrees (b) 90 degrees (c) 180 degrees on a substrate

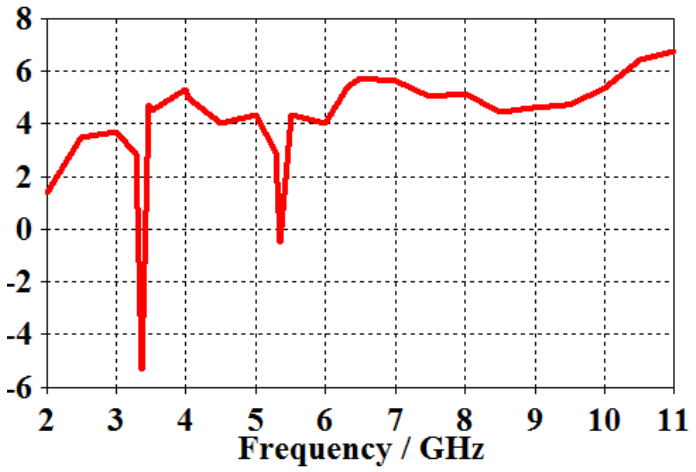

(a)

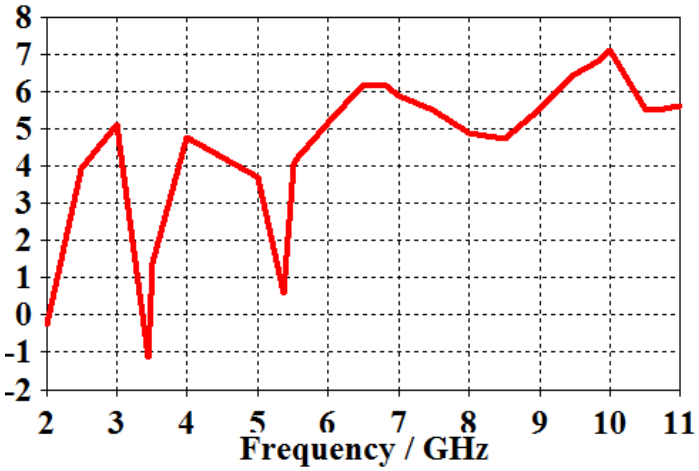

(b)

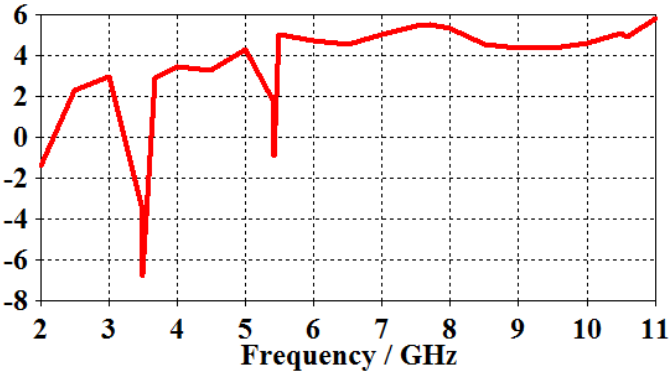

(c)

Figure 5. 22 Simulated gain vs. frequency curve of antennas placed (a) 0 degrees (b) 90 degrees (c) 180 degrees on a substrate

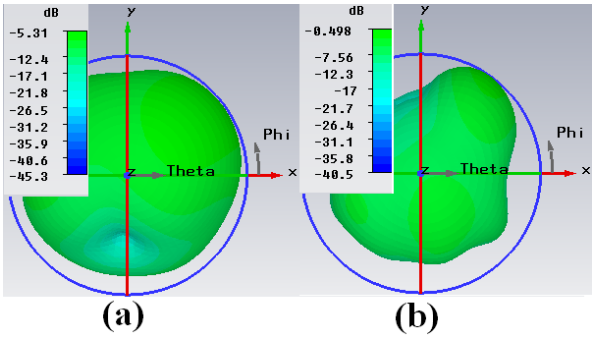

(a) 3.368 GHz (b) 5.348GHz

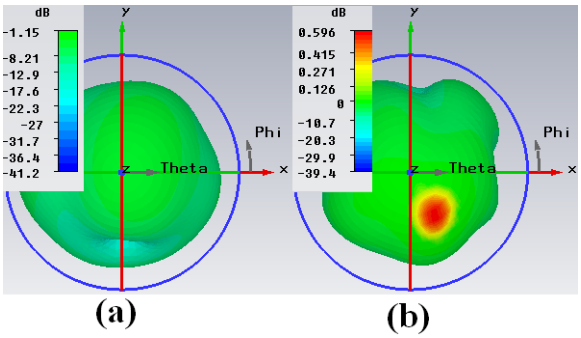

(a) 3.44GHz (b) 5.375 GHz

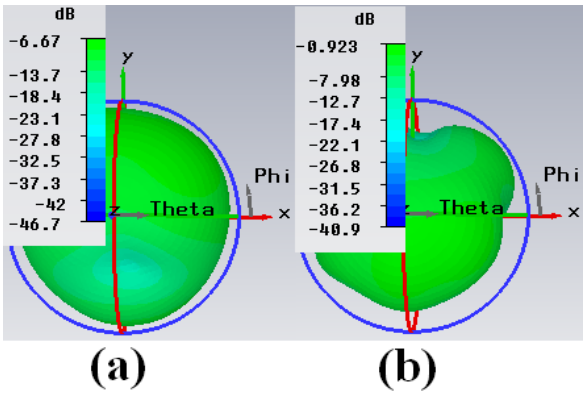

(a) 3.503GHz (b) 5.42GHz

Figure 5. 23 Simulated 3D radiation pattern of the proposed antennas at notch frequencies placed (a) 0 degrees (b) 90 degrees (c) 180 degrees on a substrate

achieved is 5.95 dB when the antennas are placed parallel to each other. The 3D-Radiation patterns at the resonant notch frequencies are shown in Fig.23. It depicts that at these frequencies the system in non-responsive.

Total active reflection coefficient (TARC)

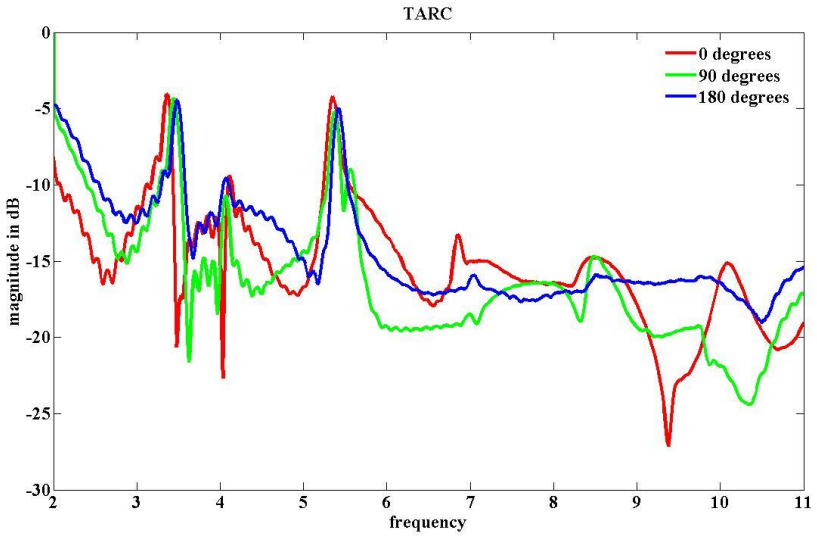

Figure 5. 24 TARC for three antenna systems

The plot is shown in Fig. 5.24 and here, this parameter is evaluated for by considering 21 excitations with θ phases from 0 to 2π.

Envelope Correlation and Capacity loss:

Fig. 5.25 depicts the envelope correlation plot over the frequency range. Typically, it is considered that antennas with less than 0.7 correlation are capable of providing substantial diversity performance [53]. From the Fig. 5.25 it is observed that the system having less correlation when the antennas are placed orthogonal to each other and the coefficient is less than 0.02 is achieved and this is quite suitable. But, when the antennas are placed 180 degrees on the substrate the achieved coefficient is less than 0.5 which is quite high compared to orthogonal system. As number of antennas increased the capacity also increases. A loss of capacity is induced by the correlation between the antennas

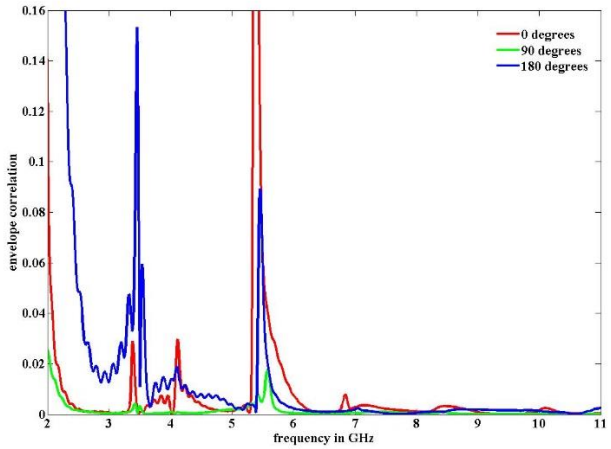

Figure 5. 25 Calculated envelope correlation coefficient for three antenna systems

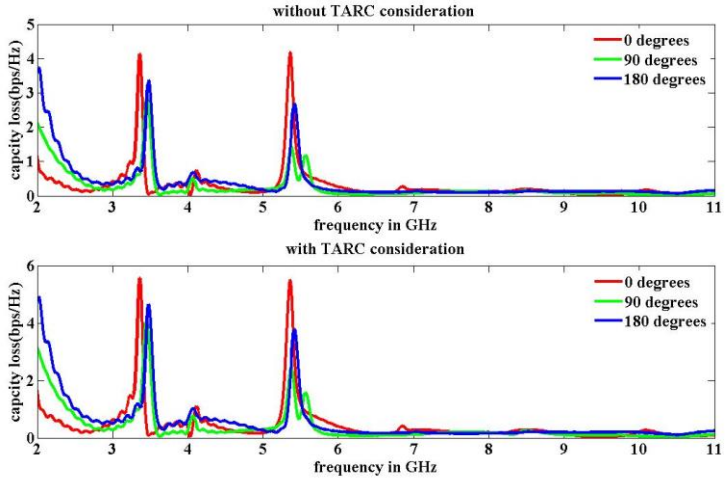

Figure 5. 26 Calculated Capacity Loss for three antenna systems

Fig. 5.26 shows the capacity loss considering with and without TARC for the proposed antenna system. As shown in Fig. 5.25, the lowest correlation cause the lowest capacity loss. From the Fig. 5.26 it is observed that capacity loss increasing as we move from 0 degrees to 180 degrees and except at the concern notch frequency range the capacity loss achieved below 0.5 bps/Hz when the antennas are placed orthogonal to each other.

CHAPTER 6

CONCLUSION AND FUTURE WORK

The results and highlights of the research work carried out are presented in this chapter. This is followed by few suggestions for future work.

Conclusions

In this work, Ultra wide band antenna geometries are designed and implemented. For this, two single patch antennas are designed for Ultra wide band applications by considering the notch for one of the antenna. The MIMO antennas are designed by using these simple geometries by placing the antenna elements in three different angular positions.

The conclusions are as follows:

a) Ultra-Wide band behavior of the antenna using lotus shaped geometry is successfully achieved.
b) Two Notch bands are successfully achieved by using two slots in the design to avoid interference at desired frequencies.
c) Fractional bandwidth greater than 120% is achieved for Ultra wide band antenna.
d) The MIMO antenna systems are designed and maximum isolation is achieved by using the fork like design on ground plane.
e) The MIMO antenna systems are designed with notch bands to avoid the interference at desired frequencies.
f) Different parameters like S11, mutual coupling, gain, capacity loss, correlation coefficient and TARC etc. are simulated and obtained for designed antennas.
g) The theoretical and simulated return loss parameter are verified by measuring those antennas.

All the presented designs are simulated using CST Microwave Studio Suite12. Designs are made using FR4 substrate having ε value 4.4 and height of 1.6mm which is a low cost material and easily available in the market. Microstrip feed line of 50Ω is used in every case.

Measurement of all the antenna parameters is done using the lab facility of IISC-Bangalore. The small frequency drift seen in measurement results is produced by the error in the manufacturing and measurement.

Future Work

The following are some of views for future work:

a) FDTD can be employed to solve and implement all designs
b) Gain of the MIMO antenna systems designed is low, other techniques can be used to increase the gain of the antenna systems in future.
c) Only single structure is used for providing isolation, so in future other structures can be used for providing the isolation of the antennas.
d) In future other notches can be achieved by different slots in designs.

PUBLICATION

D.Sudarshan, S.K.Behera, "Compact Lotus Shape Planar Microstrip Patch Antenna for UWB Application", accepted in Applied Electromagnetics Conference (AEMC), 18-20th Dec. 2013.

REFERENCES

1. Young Man Kim, “Ultra Wide Band (UWB) Technology and Applications”, NEST group, The Ohio State University, July 10, 2003.
2. G.Brzezina, "Planar Antennas in LTCC Technology for Ultra-Wideband Applications," M.A.Sc. Thesis, Carleton University, Canada, 2005.
3. J.Powell, "Antenna Design for Ultra Wideband Radio," M. A. Sc. Thesis, Massachusetts Institute of Technology, USA, May 2004.
4. Z.Chen, T. See and X.Qing, "Small Printed Ultra Wideband Antenna with Reduced Ground Plane Effect," IEEE Transactions on Antennas and Propagation, vol. 55, pp. 383-388, February 2007.
5. C. A. Balanis, “Antenna Theory - Analysis and Design,” 2nd edition, John Wiley.
6. W. F. Richards, Y. T. Lo, and D. D. Harrison, “An Improved Theory of Microstrip Antennas with Applications,” IEEE Trans. Antennas Propagat., Vol. AP-29, No. 1, pp. 38–46, January 1981.
7. D. H. Schaubert, F. G. Farrar, A. Sindoris, and S. T. Hayes, “Microstrip Antennas with Frequency Agility and Polarization Diversity,” IEEE Trans. Antennas Propagat., Vol. AP-29, No. 1, pp. 118–123, January 1981.
8. P. Bhartia and I. J. Bahl, “Frequency Agile Microstrip Antennas,” Microwave Journal, pp. 67–70, October 1982.
9. W. F. Richards and Y. T. Lo, “Theoretical and Experimental Investigation of a Microstrip Radiator with Multiple Lumped Linear Loads,” Electromagnetics, Vol. 3, No. 3–4, pp. 371–385, July–December 1983.
10. W. F. Richards and S. A. Long, “Impedance Control of Microstrip Antennas Utilizing Reactive Loading,” Proc. Intl. Telemetering Conf., pp. 285–290, Las Vegas, 1986.
11. W. F. Richards and S. A. Long, “Adaptive Pattern Control of a Reactively Loaded, Dual-Mode Microstrip Antenna,” Proc. Intl. Telemetering Conf., pp. 291–296, Las Vegas, 1986.
12. M. P. Purchine and J. T. Aberle, “A Tunable L-Band Circular Microstrip Patch Antenna,” Microwave Journal, pp. 80, 84, 87, and 88, October 1994.

13. S.D. Assimonis, T.V. Yioultsis, and C. S. Antonopoulos, "Design and Optimization of Uniplanar EBG Structures for Low Profile Antenna Applications and Mutual Coupling Reduction," IEEE Trans. Antennas Propag., vol. 60, no. 10, pp. 4944–4949, Oct. 2012.
14. J.Itoh, N.Michishita, and H. Morishita, "A study on mutual coupling reduction between two inverted-F antennas using mushroom-type EBG structures," in Proc. IEEE Antennas Propag. Soc. Int. Symp., July. 2008, pp. 1–4.
15. M.S.Sharawi, A.B.Numan, M.U.Khan, and D.N.Aloi, "A Dual-Element Dual-Band MIMO Antenna System with Enhanced Isolation for Mobile Terminals, "IEEE Antennas Wireless Propag. Lett., vol. 11, pp. 1006–1009, 2012.
16. F.-G.Zhu, J.-D.Xu, and Q.Xu, "Reduction of mutual coupling between closely-packed antenna elements using defected ground structure," Electron. Lett , vol. 45, no. 12, pp. 601–602, 2009.
17. S.Zhang, B.K.Lau, A. Sunesson and S.He, "Closely- Packed UWB MIMO / Diversity Antenna with different patterns and polarizations for USB Dongle applications," IEEE Trans. Antennas Propag., vol. 60, no. 9, pp.4372–4380, Sep. 2012.
18. T.S.P.See and Z.N. Chen, "An ultrawideband diversity antenna," IEEE Trans. Antennas Propag., vol. 57, no. 6, pp. 1597–1605, Jun. 2009
19. S.Hong, K.Chung, J. Lee, S. Jung, S.S.Lee, and J.Choi, "Design of a diversity antenna with stubs for UWB applications," Microw. Opt. Technol. Lett., vol. 50, no. 5, pp. 1352–1356, 2008.
20. G. M. Chi, B. H. Li, and D. S. Qi, "Dual-band printed diversity antenna for 2.4/5.2GHz WLAN application," Microwave Opt. Techno. Lett., vol. 45, no. 6, pp. 561-563, 2005.
21. S. Zhang, G. H. Huff, J. Feng, and J. T. Bernhard, "A pattern reconfigurable microstrip parasitic array," IEEE Trans. Antennas Propag., vol. 52, pp. 2773–2776, Oct. 2004.
22. H. Aïssat, L. Cirio, M. Grzeskowiak, et al., "Reconfigurable circularly polarized antenna for short-range communication systems," IEEE Trans.Microw. Theory Tech., vol. 54, pp. 2856–2863, Jun. 2006.
23. F. Yang and Y. Rahmat-Samii, "A reconfigurable patch antenna using switchable slots for circular polarization diversity," IEEE Microw. Wireless Compon. Lett., vol. 12, pp. 96–98, Mar. 2002.

24. Ali Imran , Yuan Duroc , F. A. Leao and Smail Tedjini, “Novel Co-located Antennas System for UWB-MIMO Applications”, IEEE Trans. Antennas Propag, pp.368-371,2009.
25. G. A. Deschamps, “Microstrip Microwave Antennas,” 3rd USAF Symposium on Antennas, 1953.
26. H. Gutton and G. Baissinot, “Flat Aerial for Ultra High Frequencies,” French Patent no. 703 113, 1955.
27. Lee, K. F., Chen, W., Advances in Microstrip and Printed Antennas, Wiley, 1997.
28. D. M. Pozar, “Microstrip Antennas,” Proc. IEEE, vol. 80, no. 1, January 1992, pp.79-81.
29. J. C Liu, B. H. Zeng, H. L. Chen, S. S. Bor and D. C. Chang, “Compact Fractal Antenna with Self-Complimentary Hilbert Curves for WLAN Dual-band and Circular Polarization Applications,” *Microwave and Optical Technology Letters*, vol. 52, no. 11, November 2010, pp. 2535-2539.
30. D. M. Pozar and B. Kaufman, “Increasing the Bandwidth of a Microstrip Antenna by Proximity Coupling,” Electronic Letters, Vol. 23, pp. 368–369, April 1987.
31. D. M. Pozar, “Microstrip Antennas,” Proc. IEEE, Vol. 80, No. 1, January 1992.
32. A. Taflove and M.E. Brodwin, “Numerical solution of steady-state electromagnetic scattering problems using the time-dependent Maxwell’s equations,” IEEE Micro. Theo. Tech., vol. MTT-23, no. 8, Aug. 1975, pp. 623–630.
33. A. Taflove and K. Umashankar, “A hybrid moment method/finite-difference time-domain approach to electromagnetic coupling and aperture penetration into complex geometries,” IEEE Trans. Ant. Prop., vol. AP-30, no. 4, July1982, pp. 617–627. Also in B. J. Strait (ed.), Applications of the Method of Moments to Electromagnetic Fields. Orlando, FL: SCEE Press, Feb. 1980, pp. 361–426.
34. M. Okoniewski, “Vector wave equation 2D-FDTD method for guided wave equation,” IEEE Micro. Guided Wave Lett., vol. 3, no. 9, Sept. 1993, pp. 307– 309.
35. A. Taflove and K.R. Umashankar, “The finite-difference time-domain method for numerical modeling of electromagnetic wave interactions,” Electromagnetics, vol. 10, 1990, pp. 105–126.
36. M.N.O. Sadiku, V. Bemmel, and S. Agbo, “Stability criteria for finite difference time-domain algorithm,” Proc. IEEE Southeastcon, April 1990, pp. 48–50.

37. Matthew N. O. Sadiku, “Numerical Techniques in Electromagnetics,” 2nd edition, CRC Press.
38. Federal Communications Commission, First report and order, revision of Part 15 of Commission’s rule regarding ultra-wideband transmission system FCC 02-48, Washington, DC, April 2002
39. K.L. Wong, “Compact and broadband microstrip antennas” (John Wiley & Sons, 2002)
40. C.K. Wu, K.L. Wong, “Broadband microstrip antenna with directly coupled and gap-coupled parasitic patches”, Microw. Opt. Technol. Lett., 1999, vol. 22, no. 5, pp. 348–349
41. T. Huynh, K.F. Lee, “Single-layer single-patch wideband microstrip antenna”, Electron. Lett., 1995, vol. 31,no. 3, pp. 1310 –1311
42. K.L. Wong, W.H. Hsu: “A broadband rectangular patch antenna with a pair of wide slits”, IEEE Trans. Antennas Propag., 2001, vol. 49, pp. 1345 –1347
43. J. Lao, R. Jin, J. Geng, Q. Wu, “An ultra-wideband microstrip elliptical slot antenna exited by a circular patch”, Microw. Opt. Technol. Lett., 2008, vol. 50, no. 4, pp. 845–846
44. A.C. Azenui, H.Y.D. Yang, “A printed crescent patch antenna for ultrawideband applications”, IEEE Antennas Wirel. Propag. Lett., 2007, vol. 6, pp. 113 –116
45. E.S. Angelopoulos, A.Z. Anastopoulos, D.I. Kaklamani, A.A. Alexandridis, F. Lazarakis, K. Dangakis, “Circular and elliptical CPW-fed slot and microstrip-fed antennas for ultrawideband applications”, IEEE Antennas Wirel. Propag. Lett., 2006, vol. 5, pp. 294 –297
46. T.A. Denidni, M.A.Habib, “Broadband printed CPW-fed circular slot Antenna”, Electron. Lett., 2006, vol. 42,no. 3, pp. 135–136
47. Trang Dang Nguyen, Dong Hyun Lee, and Hyun Chang Park,” Design and analysis of compact printed triple band-notched UWB antenna”, IEEE antenna and wireless propagation Lett., 2011, vol. 10, pp. 403-406.
48. S. H. Choi, J. K. Park, S. K. Kim and J. Y. Park. "A new ultrawideband antenna for UWB applications," Microw. Opt. Tech. Lett., vol. 40, no. 5, pp. 399-401. 2004.

49. D.W. Browne, M. Manteghi, M.P. Fitz, and Y. Rahmat-Samii, Experiments with compact antenna arrays for MIMO radio communications, IEEE Trans Antennas Propag 54 (2006), 3239–3250.
50. S.-H. Chae, S. Oh, and S.-O. Park, Analysis of mutual coupling, correlations, and TARC in WiBro MIMO array antenna, IEEE Antennas Wireless Propag Lett 6 (2007), 122–125.
51. S. Blanch, J. Romeu, and I. Corbella, Exact representation of antenna system diversity performance from input parameter description, Electron Lett 39 (2003), 705–707.
52. J. Thaysen and K.B. Jakobsen, Envelope correlation in (N,N) MIMO antenna array from scattering parameters, Microwave Opt Technol Lett 48 (2006), 832–834.
53. I. Salonen and P. vainikainen, "Estimation of signal correlation in antenna arrays," in Proc. of the 12th Int. Symp. on Antennas (JINA 2002), Nice, France, vol. 2, 2002, pp. 383-386.
54. H. Shin and J.H. Lee, Capacity of multiple-antenna fading channels: spatial fading correlation, double scattering, and keyhole, IEEE Trans Inform Theory 49 (2003), 2636–2647.

Online Sources:

1) http://www.edaboard.com/
2) http://www.antenna-theory.com/
3) https://www.wikipedia.org/
4) www.google.com